PNNL-34160
M3LW-23OR0404023

Light Water Reactor Sustainability Program

Frequency Domain Reflectometry (FDR) Simulation Techniques for Digital Twin Representation of an Electrical Cable

April 2023

U.S. Department of Energy

Office of Nuclear Energy

PNNL-34160
M3LW-23OR0404023

Frequency Domain Reflectometry (FDR) Simulation Techniques for Digital Twin Representation of an Electrical Cable

M.P. Spencer, S.W. Glass, A. Sriraman, M. Prowant,
J. Tedeschi, J. Son, L.S. Fifield
Pacific Northwest National Laboratory

April 2023

Prepared for the
U.S. Department of Energy
Office of Nuclear Energy

SUMMARY

Simulation of nuclear electric cable system response to frequency domain reflectometry (FDR) tests can be instrumental to understanding results of these tests and the nature and influence of various cable anomalies on test signatures. Reflectometry simulations are based upon a finite element representation of cable conductors (in a multi-conductor cable) and insulation to produce an S-parameter at each evaluated frequency. The aggregate collection of cable S-parameters can simulate the influence of a test signal injected into a physical cable. Such an approach was undertaken in this work to produce a digital twin simulation of a low-voltage electrical cable. The electrical cable digital twin examined the influence of test simulation parameters and the relative influence of cable anomalies, including thermal aging, water or moisture exposure, water or moisture ingress, and other anomalies. The digital twin in this work included modeling of the conductors, insulation, jacket, and surrounding environment (air, water, etc.). The digital twin could be expanded to include cable bends, junctions and splices, branch or "T" systems, and termination impedances of connected motors or instruments. Observations and conclusions of this work include:

1. 3D digital twin simulation of an electrical cable using an FDR approach is feasible, but there are tradeoffs between simulation fidelity and solution run time that must be balanced to ensure the simulation solves in a practical period of time (e.g., less than 20 minutes). Parameters to balance in this tradeoff include frequency bandwidth, number of frequencies, mesh density, connection impedance, and permittivity variance.

2. The digital twin simulation can explain FDR sensitivity to various cable anomalies, including entry and exit from an oven or water bath.

3. The digital twin simulation FDR response attenuates with distance along the cable and is further affected by the frequency bandwidth, similar to the response observed with physical measurements.

4. The resolution of the digital twin FDR peaks increases with increasing bandwidth and with increasing number of frequencies, again similar to physical measurements.

5. The presence of multiple anomalies in the digital twin does not substantially attenuate the FDR response beyond the first encountered anomaly and impedance mismatch.

6. Spectral variation of the permittivity does not have a significant effect on the FDR response compared to a fixed nominal permittivity value.

7. Extension of the digital twin to 1000 ft still allows for detection of distal anomalies near the far end of the electrical cable from the instrument connection point.

8. The ARENA test bed facilitates efficient nondestructive evaluation of well understood cable anomalies with various condition monitoring methods without risking actual plant system damage.

It is anticipated that electrical cable system digital twins, such as the one described here, will enable development of increasingly sophisticated and effective condition monitoring and prediction tools to support continued safe and efficient operation of light water reactors.

ACKNOWLEDGEMENTS

This work was sponsored by the U.S. Department of Energy, Office of Nuclear Energy, for the Light Water Reactor Sustainability (LWRS) Program Materials Research Pathway. The authors extend their appreciation to Pathway Leads Dr. Thomas Rosseel and Dr. Xiang (Frank) Chen for LWRS programmatic support. This work was performed at the Pacific Northwest National Laboratory (PNNL). PNNL is operated by Battelle for the U.S. Department of Energy under contract DE-AC05-76RL01830.

CONTENTS

FIGURES

TABLES

ACRONYMS

ARENA	Accelerated and Real-Time Environmental Nodal Assessment
AWG	American wire gauge
a.u.	arbitrary units
CPE	chlorinated polyethylene
DBE	design-basis event
DFT	distance-to-fault
DOE	Department of Energy
EAB	elongation at break
EPR	ethylene-propylene rubber
EPRI	Electric Power Research Institute
FDR	frequency domain reflectometry
FFT	fast Fourier transform
IAEA	International Atomic Energy Agency
LWRS	Light Water Reactor Sustainability Program
NDE	nondestructive evaluation
NPP	nuclear power plant
PNNL	Pacific Northwest National Laboratory
SLR	subsequent license renewal
SSTDR	spread spectrum time domain reflectometry
TDR	time domain reflectometry
VAC	volts alternating current
VNA	vector network analyzer
VOP	velocity of propagation

1. INTRODUCTION

This report is submitted in fulfillment of the deliverable for the LWRS Milestone Report (M3LW-22OR0404023) for nondestructive examination (NDE) of cables and cable insulation. The work is part of an overall effort to develop a technical basis for assessing the level and impact of cable insulation aging and degradation in nuclear power plants (NPPs). Previous related work has included:

- Test-bed development (Glass et al. 2023)
- Effect of thermal aging (Glass et al. 2022)
- Moisture detection (Glass et al. 2021)
- Environmental stressors (Glass et al. 2017), and
- Bulk assessment approaches (Glass et al. 2016)

1.1 Motivation

Nearly 20% of the electricity produced in the U.S. comes from NPPs (Joskow 2006). NPPs were originally qualified for an operational lifetime of 40 years (Subudhi 1996; Gazdzinski et al. 1996). However, a majority of U.S. NPPs have applied for and been granted 20-year extensions following the original license period. With many NPPs preparing for an additional 20-year subsequent license renewal (SLR), it is critical to ensure the continued safe operation of NPPs during the extended license periods. Therefore, it is important to evaluate how the characteristics and performance of materials installed in aging plant components change over time. Such information is used in the development of aging management programs to ensure the continued safe operation of NPPs under normal and design-basis events (DBE).

Within NPPs, electrical cables are susceptible to aging and degradation with hundreds of miles in nuclear containment alone. These cables are commonly low-voltage, critical infrastructure required for power, control, and instrumentation associated with safety and operational systems (Blocker et al. 1996), and may be exposed to environmental stressors, such as elevated temperature, moisture, and gamma radiation. Such stressors can cause degradation and eventual failure of electrical cables, which may lead to loss of safety systems if not detected and managed through the plant aging management programs (IAEA 2012). Practically all utilities include some form of cable NDE in their aging management program since performance testing to assure acceptable cable function is more cost effective than replacing all cables that exceed their qualified life. Even so, utilities are continually working to improve test quality and reduce costs associated with their cable NDE programs.

Given the large volume of different types of electrical cables servicing NPPs, versatile prevention and detection of electrical cable failure during the operating lifetime of an NPP is a vital part of aging management. To evaluate the degradation of electrical cables, and particularly the interaction of electrical cable test technologies with various damage mechanisms, PNNL developed the Accelerated and Real-time Environmental Nodal Assessment (ARENA) test bed (Glass et al. 2023), see Figure 1-1. The vision behind creation of this facility is to establish a one-stop modular test facility that allows for implementation of a broad range of test methods to detect faults and anomalies in a variety of cables and systems in a controlled environment. The goal is to assess the effectiveness of cable diagnostic and monitoring techniques safely and reliably in scenarios of interest to utilities, such as high-stress environments, elevated temperatures, electrical failures, moisture ingress, and more. The ARENA test bed features:

- A 3-phase 480 VAC motor,
- A large thermal aging oven with inlet and outlet ports for thermal aging studies,
- An approximately 1-m water trough to facilitate moisture ingress evaluation,
- Elevated cable trays to minimize disturbance to the electrical cables during testing,

- High sensitivity ground-fault circuit breaker technology to protect line circuit from faults,
- Remote control start and stop to protect personnel from arc-flash hazards,
- Electrical cable taps for instruments both near the controller and near the motor.

The ARENA test bed also supports coupling of off-line de-energized and on-line energized cable NDE techniques, such as electrical reflectometry (frequency domain reflectometry, time domain reflectometry, and spread-spectrum time domain reflectometry) (Glass et al. 2017), tan delta (Glass et al. 2020), and dielectric spectroscopy (Imperatore et al. 2017). While NDE techniques have seen growth and improvement in cable diagnostics and fault detection performance, current implementation of NDE has notable limitations. First, there is no single NDE method to comprehensively evaluate cable performance and safety, and therefore multiple bulk, distributed, and local tests may be required to collectively provide reliable assessment of electrical cable performance (Glass et al. 2015). Second, most of the widespread NDE techniques (frequency domain reflectometry, tan delta, and dielectric spectroscopy) require electrical cables to be powered down and/or disconnected on at least one end to implement the test, which risks faulty re-termination errors and may ultimately result in higher operation and maintenance costs. Consequently, to improve the efficiency and cost-effectiveness of electrical cable testing, utilities are constantly seeking alternative ways to implement fewer and more robust NDE techniques for electrical cable assessment. One potential tool to better understand cable system degradation is a simulated electrical cable digital twin, which could be used to model degradation of cable systems in real-time without the need of physically coupling to electrical cables. Consequently, this work seeks to evaluate an NDE digital twin for electrical cables based upon frequency domain reflectometry (FDR).

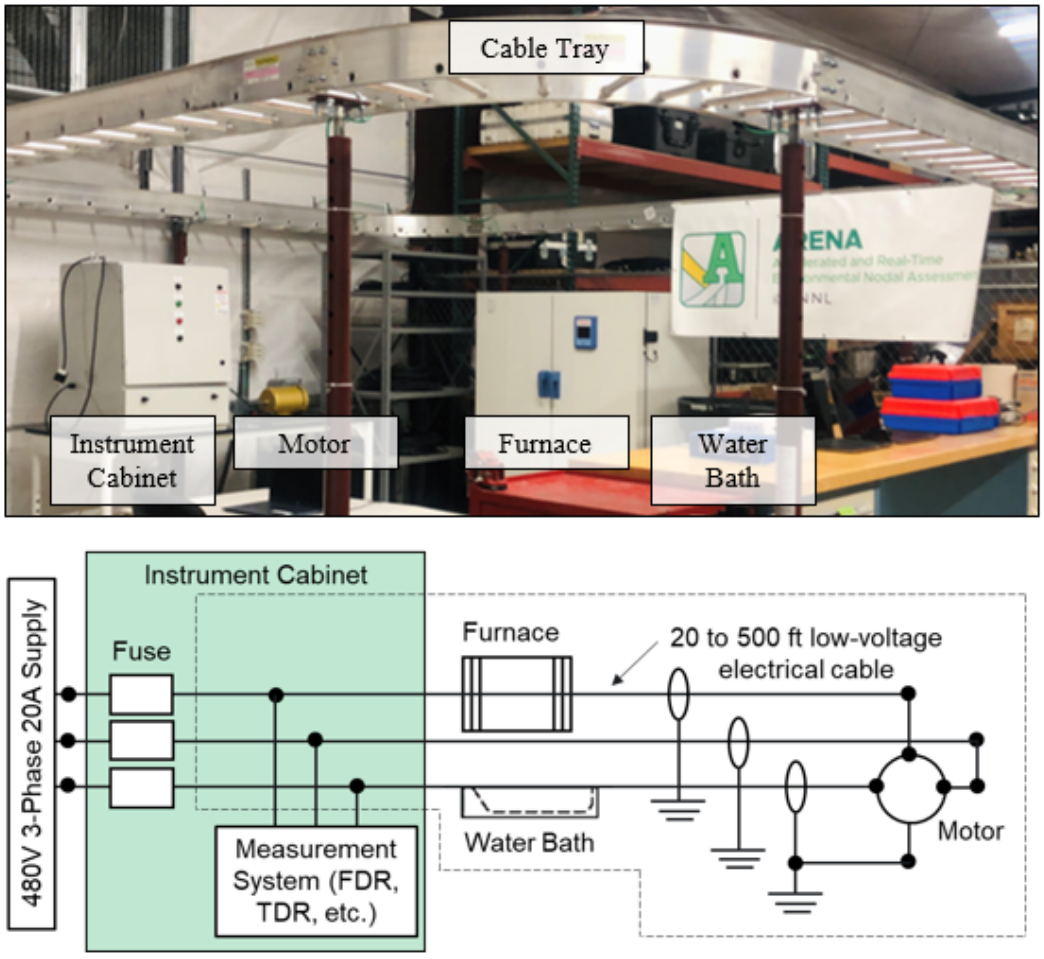

Figure 1-1. The ARENA test bed (top) digital image and (bottom) schematic (Glass et al. 2023).

1.2 Background

Broadly, reflectometry is a non-destructive technique that is based on the reflection of electromagnetic waves at surfaces and/or interfaces to locate changes and characterize various objects. Within the realm of electrical characterization, reflectometry techniques may be physically applied to nondestructively conduct distance-to-fault (DTF) measurements on electrical cables and wires. For FDR measurements, the steady-state amplitude and phase of the reflected signal is built up over numerous discrete frequencies. A similar approach can be carried out for digital twins where a discrete combination of frequency-based simulations is carried out to replicate electromagnetic reflection within electrical cables.

1.2.1 Digital Twins

While the definition of a digital twin, also known as a virtual twin, can vary widely, a commonly accepted definition is,

> "*a digital representation of a real-world entity or system. The implementation of a digital twin is encapsulated software object or model that mirrors a unique physical object, process, organization, person, or other abstraction*" (Gartner Glossary 2023).

Thus, a digital twin is the simulation of a real-world object with real-world inputs. More specifically, a digital twin has three components: a physical object and its environment, digital representation of the object, and communication between the two (Wikipedia 2023). A potential framework for evaluating digital twins are the five levels of achievement:

L1) Basic digital twin that can be connected to the physical world,
L2) Digital twin with real-time feedback and control,
L3) Digital twin with predictive analytics and maintenance,
L4) Digital twin with a range of probabilities and uncertainties, approaching autonomy,
L5) Digital twin that is intelligent and autonomous.

In this work, we aim to demonstrate the basic functionality of an FDR electrical cable digital twin including the conductors and shield (if present), insulation, jacket, and surrounding environment (air, water, etc.). As such, we are working towards the first level of achievement (L1). Further expansion of the simulation could include cable bends, splices and terminations, thermal effects, cable "Ts" and branches, and effects of insulation parameters.

1.2.2 Frequency Domain Reflectometry

FDR is a nondestructive electrical inspection technique used to detect, localize, and characterize subtle impedance changes in power and communication system conductors and insulation materials along the length of a cable from a single connection point. FDR is based on the interaction of electromagnetic waves with conductors and dielectric materials as the waves propagate along the cable. The technique uses the principles of transmission line theory to locate and quantify impedance changes in the cable circuit. These impedance changes can result from connections, faults in the conductors, or degradation in the cable polymer material (Furse et al. 2003).

For an FDR measurement, two conductors in the cable system are treated as a transmission line through which a low-voltage swept-frequency waveform is propagated. A linearly increasing "chirp" sinusoidal waveform is the typical excitation signal used in the FDR technique. The excitation signal can be generated for transmission into the cable using an analog circuit, such as a voltage-controlled oscillator, or using a digital circuit such as a direct digital synthesizer. As the excitation signal is swept over the frequency range and the associated electromagnetic wave travels down the cable, the impedance response, or more

specifically the reflected complex voltage, is recorded at each frequency to characterize wave interaction with the conductors and surrounding dielectric materials. The remote end of the cable can be terminated in an arbitrary impedance different from the cable characteristic impedance but is often grounded or open-circuited during testing. Because the applied signal is low-voltage, the test is nondestructive and poses no special safety concerns to operators assuming that routine electrical safety procedures are followed (Glass et al. 2017). In most cases, it is only necessary to de-energize the cables and de-termination is not required, but typically at least one end of the cabling is de-terminated to connect the FDR system.

1.3 Objective

The primary objective of this work is to evaluate and confirm the response of a 3D FDR electrical cable digital twin. As a first step, the digital twin was developed towards the first level of achievement, namely demonstrating that the digital twin can be connected to the physical world.

2. MATERIALS AND METHODS

To achieve the objectives of this work, comparisons were made to thermal aging experiments performed at PNNL (Glass et al. 2022) and those in literature (Sriraman et al. 2018). Therefore, materials and their properties selected for the digital twin were based upon physical testing as discussed below.

2.1 Materials

A low-voltage, tri-core, non-shielded electrical cable manufactured by General Cable® (Catalog number 383830) was selected for evaluation of the electrical cable digital twin. Details regarding the materials and dimensions of the cable are shown in Table 1. The cable is comprised of three 14 AWG copper conductors insulated by ethylene-propylene rubber (EPR) and protected by a chlorinated polyethylene (CPE) jacket. The cable has a voltage rating of 600V and an operating temperature rating of 90°C. A digital image of the cable cross-section is shown in Figure 2-1, along with the corresponding solid model cross-section in SolidWorks® (www.solidworks.com).

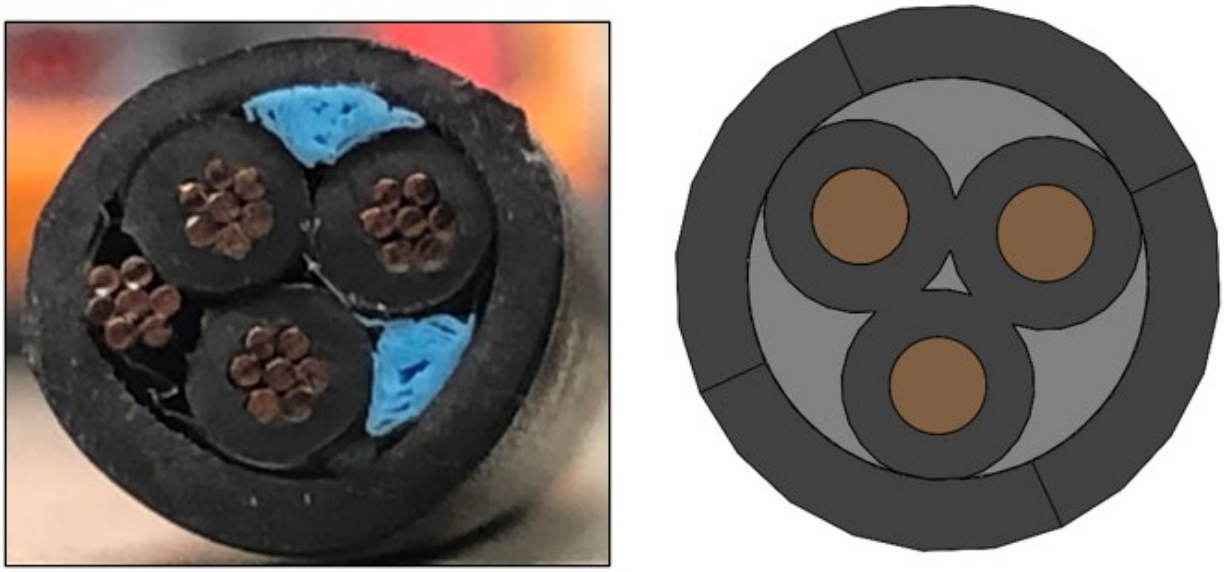

Figure 2-1. (Left) Digital image of General Cable (383830) cross-section and (right) corresponding solid model.

Table 1. Manufacturer information for the evaluated electrical cable.

Manufacturer	Jacket		Insulation		Conductor	Outer Diameter (mm)
	Material	Thickness (mm)	Material	Thickness (mm)		
General Cable (part# 383830)	CPE	1.14	EPR	0.76 (min)	14 AWG	9.91

CPE = chlorinated polyethylene; EPR = ethylene-propylene rubber.

2.2 Experimental Methods

For comparison to and validation of the electrical cable digital twin, ARENA FDR measurements were collected on the same electrical cable (General Cable 383830) undergoing thermal aging at 140°C for up to 62-days (Glass et al. 2022). In addition, the spectral permittivity of the aged sections of the cable were estimated based upon literature (Sriraman et al. 2018).

2.2.1 Thermal Aging

Accelerated thermal aging in an air-circulating oven at 140°C was used to induced thermal degradation representative of long-term aging within NPPs in the ARENA test bed (Fifield and Duckworth 2015). A length of approximately 100-ft of the General Cable electrical cable was routed from the instrument cabinet, through the overhead trays, into and out of an air-circulating oven (ThermoFisher Scientific Heratherm™ OMH-750 Advanced Protocol), and finally to a 480 VAC motor. Within the oven, an approximately 30-ft section of the cable was carefully wrapped around a mandrel as shown in Figure 2-2 (from approximately 45-to-75 ft). Accelerated isothermal aging was performed on the 30-ft cable section. FDR measurements, to be discussed next, were collected on the de-energized electrical cable at ambient conditions (oven turned off and allowed to cool for measurements) – previous work has observed a diminished FDR response when collected at elevated temperatures (Spencer et al. 2023). FDR measurements were collected at time points of 0, 3, 7, 11, 15, 19, 23, 27, 33, 37, 43, 49, 55, and 62 days of aging. For reference, relative mechanical strain at break (EAB) of insulation witness samples with the same aging time points were found to range between 110% and 65% and are also shown in Figure 2-2 (Glass et al. 2022).

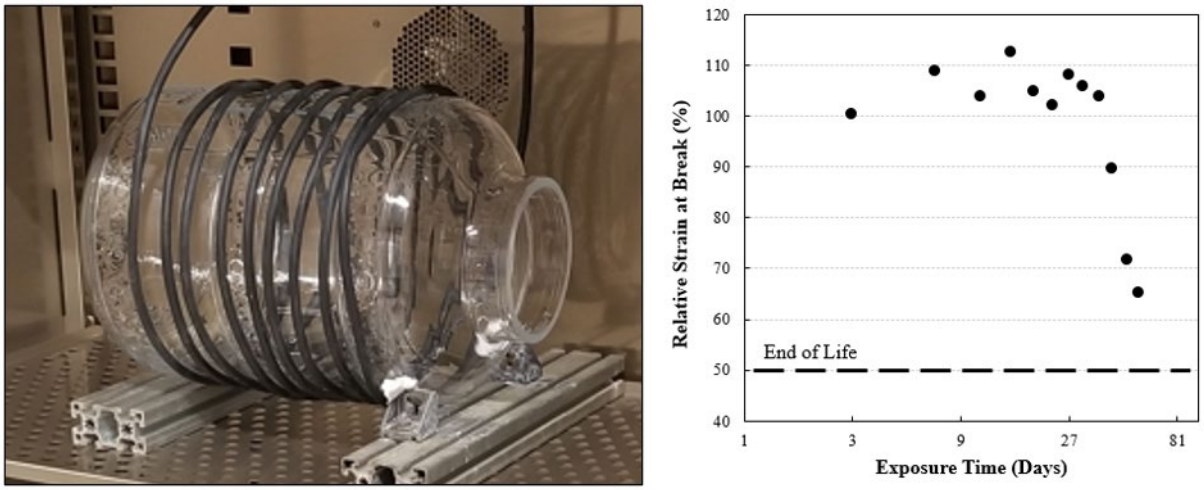

Figure 2-2. General Cable electrical cable (383830) (left) within the ARENA thermal oven wrapped around a mandrel and (right) mechanical strain at break for witness samples at the evaluated aging time points (140°C).

2.2.2 Frequency Domain Reflectometry

A compact vector network analyzer (VNA) (Copper Mountain TR1300) was used to perform FDR measurements. The frequency bandwidth for the FDR chirp signal was selected to be 300 kHz to 100 MHz, corresponding to a spatial resolution of approximately 3.3 ft. The velocity factor for the cable was set at 0.66 and the number of uniformly spaced frequency samples was set to be 1024 to ensure signal propagation down the entire length of the cable and back at the chosen bandwidth. For each FDR measurement, two of the three conductor leads of the cable were randomly selected and attached to the VNA for measurement using alligator clips. All FDR measurements were made on the de-energized (offline) cable only. The collected FDR data was then processed using Microsoft Excel wherein the data was converted to the time domain using inverse Fourier transform without any zero padding. The decibels of the reflection coefficient of the FDR signal were plotted against the length along the cable. Additional details regarding the experimental procedure can be found in our previous work (Glass et al. 2022).

2.2.3 Permittivity

Spectral permittivity of the aged insulation was estimated from literature for a similar material type (Okoguard EPR insulation) (Sriraman et al. 2018). Specifically, permittivity over the bandwidth of interest (see Section 2.3.1.4) was linearly extrapolated from the trends of Figure 2-3 for responses at 0, 49, and 70 days.

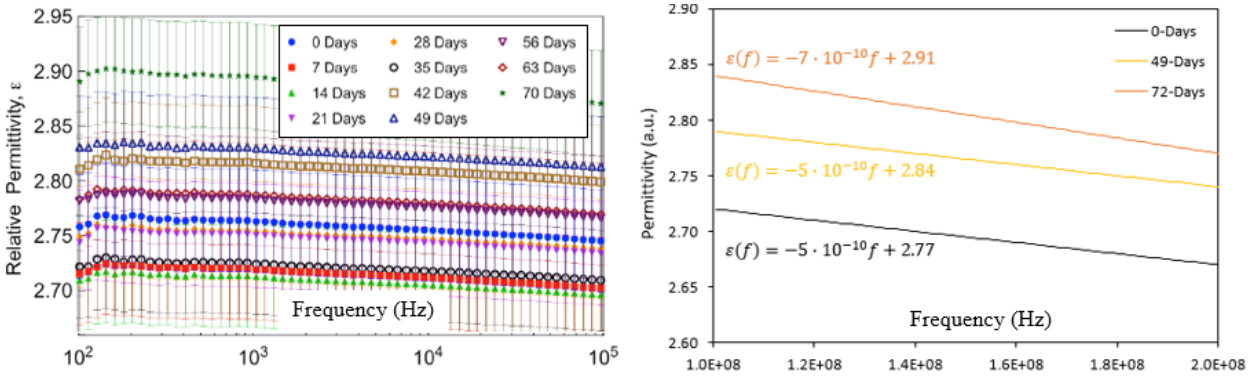

Figure 2-3. (Left) Spectral permittivity for aged Okoguard EPR insulation (Sriraman et al. 2018) and (right) extrapolated frequency-based permittivity included for comparison to ARENA test data.

2.3 Digital Twin Development

The digital twin was based upon the non-shielded, 3-conductor General Cable electrical cable reported in Table 1. The solid model of the electrical cable was developed in SolidWorks® and is shown in Figure 2-1. To simplify the geometry and avoid point contact, the thickness of the insulation was increased to 0.84 in from a minimum of 0.76 in. In addition, the stranded conductors were modeled as a single solid component. The length of the cable was selected to be 30 m (approximately 98.5 ft) to match experimental testing. Twisting was not included within the solid model and was not observed in the physical cable. Lastly, a port was connected across two of the conductors (see Figure 2-4) at both ends of the cable.

2.3.1 Baseline Digital Twin

The digital twin was developed using COMSOL Multiphysics® (www.comsol.com). The solid model was first imported into COMSOL. Next, a fluid domain (e.g., air or water) was placed internally and surrounding the cable to a diameter of 22 mm; the fluid domain surrounding the cable extended long enough to encapsulate both ports. The cable was then partitioned into 30 equally spaced segments with length of 1

m. Afterwards, a union operation was conducted such that all contacting boundaries had conforming mesh and continuity of fields or fluxes across them. The cable with the included fluid domain is shown in Figure 2-4; note that the lumped port is specified across two conductors to mimic a transmission line for FDR measurements.

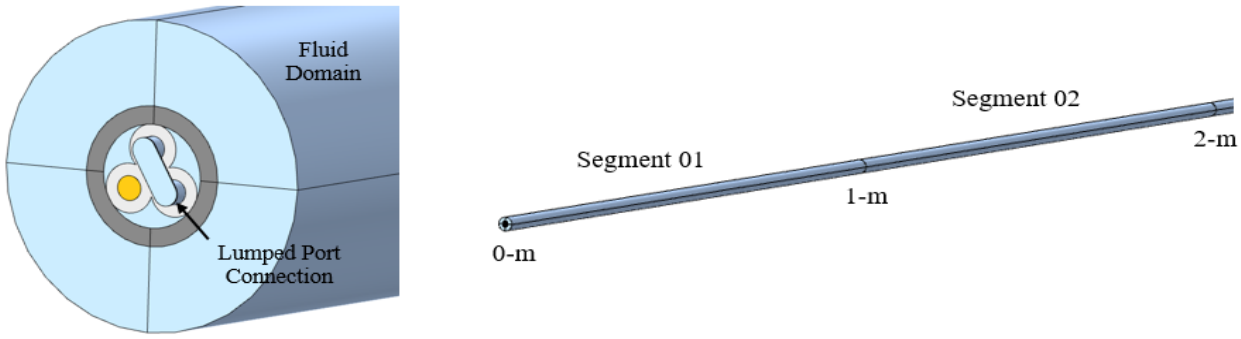

Figure 2-4. The General Cable electrical cable within COMSOL: (left) included internal and external fluid domains and (right) segmenting the cable into thirty 1 m partitions (only two shown).

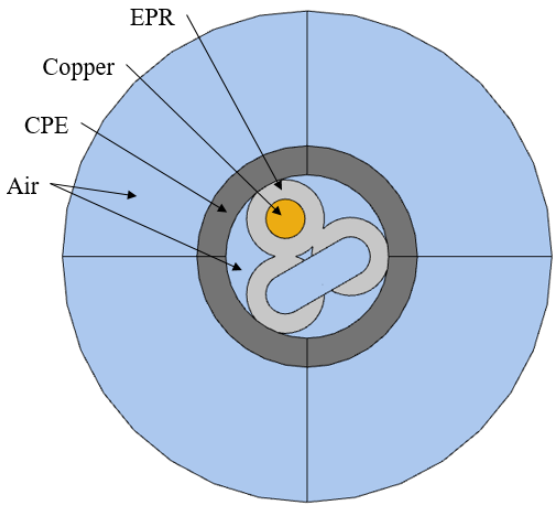

Figure 2-5. Cross-sectional view of the digital twin indicating respective materials.

2.3.1.1 Baseline Materials

The material properties of the digital twin are shown in Figure 2-5 and Table 2. The permittivity of the conductor was defined as 1.00, which is the default value for conductive materials in COMSOL (conductivity response dominates permittivity response). The permittivity of the insulation was selected to be a function of the frequency as shown in Equation (1),

$$\varepsilon = \varepsilon(f) \cdot (1 + \beta_s) \cdot \alpha_s \tag{1}$$

where $\varepsilon(f)$ is the spectral permittivity over the evaluated bandwidth and α_s and β_s represent manual damage (e.g., 1.1 for a 10% increase in permittivity) and a random constant for segment s, respectively. For the baseline digital twin, α_s was set as 1.0 for each segment. The random constant for each segment was generated using a Gaussian distribution with mean of 0.0 and standard deviation of 0.01 (www.random.org); the variance placed on permittivity for each segment will induce random noise in the time domain signal, similar to that observed with physical FDR measurements (Glass, Jones, Fifield,

Hartman, et al. 2017) and likely due to manufacturing tolerances. For simplicity, the baseline digital twin included spectral permittivity with a linear fit in the form of,

$$\varepsilon(f) = a \cdot f + b \tag{2}$$

where a and b are the slope and y-intercept of the spectral permittivity, respectively. In this work, the baseline digital twin was selected to have a equal to -1.3631×10^{-10} to mimic the response of common insulators within the MHz frequency range (Kakimoto et al. 1987) and b equal to 2.72 which is similar to the low frequency permittivity of EPR (Sriraman et al. 2018). Thus, permittivity varies from approximately 2.71 at 100 MHz to 2.69 at 200 MHz.

Table 2. Material properties of the digital twin.

Material	Relative Permeability, μ_r	Electrical Conductivity, σ (S/m)	Relative Permittivity, ε_r
Air	1.00	1.00×10^{-10}	1.00
Copper	1.00	6.00×10^{7} (Pan et al. 2022)	1.00
CPE	1.00	1.00×10^{-10}	5.65 (Sriraman et al. 2018)
EPR	1.00	1.00×10^{-10}	See above

CPE = chlorinated polyethylene; EPR = ethylene-propylene rubber.

2.3.1.2 Baseline Electromagnetic Module

To generate the FDR electrical cable digital twin, the 3D model was discretized and Maxwell's equations in the frequency domain were evaluated at each nodal location. To accomplish this, the electromagnetic waves module in the frequency domain was incorporated with linear discretization to reduce simulation time. For reference, Maxwell's equations in the frequency domain are given by Equation (3), where $\boldsymbol{E}$ is the electric field, c_0 is the speed of light in a vacuum (approximately 2.998×10^{8} m/s), ω is the angular frequency, and ε_0 is the permittivity of free space (approximately 8.854×10^{-12} F/m).

$$\nabla \times \mu_r^{-1}(\nabla \times \boldsymbol{E}) - \frac{\omega^2}{c_0^2}\left(\varepsilon_r - \frac{j\sigma}{\omega\varepsilon_0}\right)\boldsymbol{E} = \boldsymbol{0} \tag{3}$$

Within the electromagnetic waves module, a scattering boundary condition with no incident field, plane wave, and first order was first imposed on the external fluid domain surface to ensure no reflections. Next, a transition boundary condition with thickness of 0.5 mm was placed on the conductor surfaces to model losses. Third, a perfect electrical conductor boundary condition was applied to the port connection (only the cylindrical surfaces as shown in Figure 2-6). Lastly, a uniform lumped port was designated at one end of the cable (the other end acted as open-ended); here, the port was selected to be for cable terminals such that voltage could be injected (1 V at a phase angle of 0 rad with characteristic impedance of 50 Ω) and S-parameters calculated. Details regarding the boundary conditions are shown in Figure 2-6.

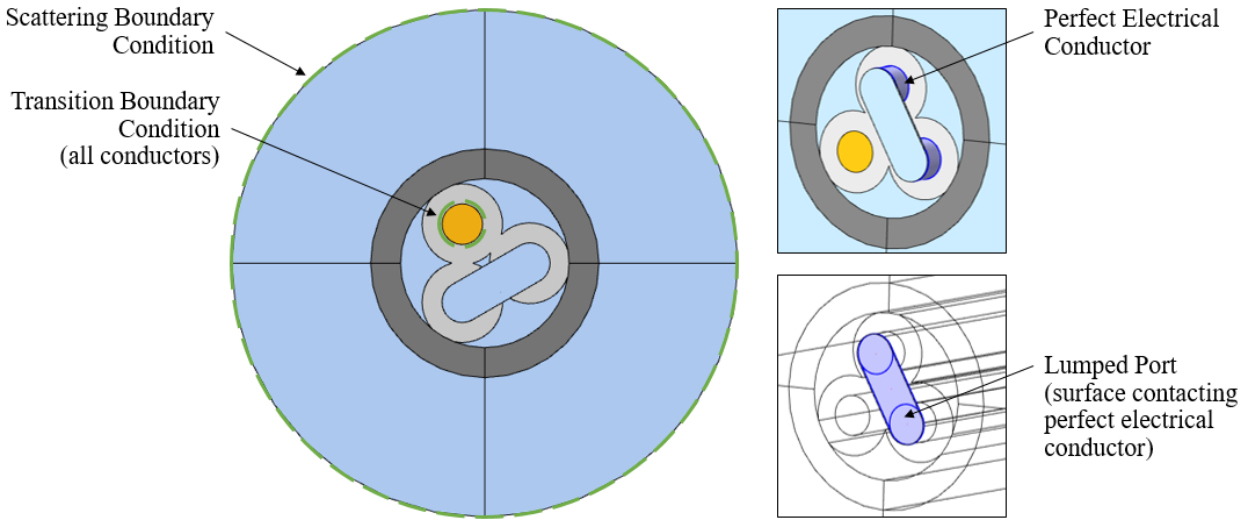

Figure 2-6. Boundary conditions included in the baseline electrical cable digital twin.

2.3.1.3 Baseline Meshing

Care was taken while meshing the digital twin domain due to incorporation of linear discretization. The cross-sectional and swept mesh of the baseline digital twin is shown in Figure 2-7. First, the mesh was mapped over the cross-section of the jacket to a maximum 0.7 mm with 2 elements across the thickness. Afterwards, the mesh was swept at a distribution of the minimum wavelength divided by 20 (or 13 distributions) for each segment. Next, the cross-sectional mesh of the external fluid domain was mapped with a symmetric distribution (linear growth rate) with 6 elements. The cross-sectional edge of each insulation segment was then specified to have 6 distributions, after which a free triangular mesh was generated on the cross-section for the internal fluid domain, insulation, and conductors. Following this, the cross-sectional mesh for the conductors, insulation, and internal and external fluid domain were swept for the entire digital twin domain. A free tetrahedral mesh was then specified for the remaining domains. The resulting mesh had 313829 elements with an average skewness quality of approximately 0.84 (with 1.00 representing a perfectly regular element).

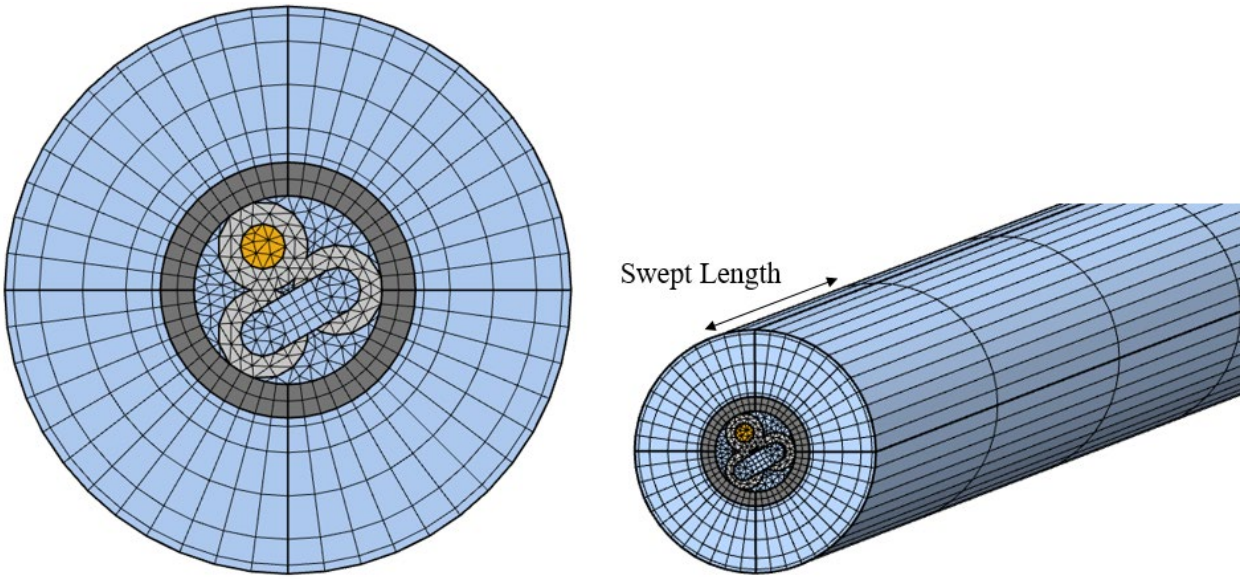

Figure 2-7. Mesh of the baseline electrical cable digital twin.

2.3.1.4 Baseline Response

The baseline digital twin was solved in the frequency domain from 100 MHz to 200 MHz (100 MHz bandwidth) with 64 uniformly spaced frequencies. To accomplish this, 64 independent simulations were run in sequence at each frequency with the output of each simulation being the reflection coefficients (real and imaginary) calculated at the lumped port. The time to solution to evaluate all frequencies was less than 20 minutes for the baseline digital twin and the total file size was less than 100 MB (with outputs only specified at lumped port). The output Touchstone file was evaluated following the procedure described above for evaluation of FDR data (namely, conversion from frequency to time domain - see our previous work (Glass et al. 2021)). The time domain response of the baseline digital twin is shown in Figure 2-8 with a velocity factor of 0.65, similar to the FDR time domain response of an undamaged electrical cable (Glass et al. 2017). More specifically, the connection and open end were captured in the digital twin, along with variations in the response due to tolerance placed on permittivity.

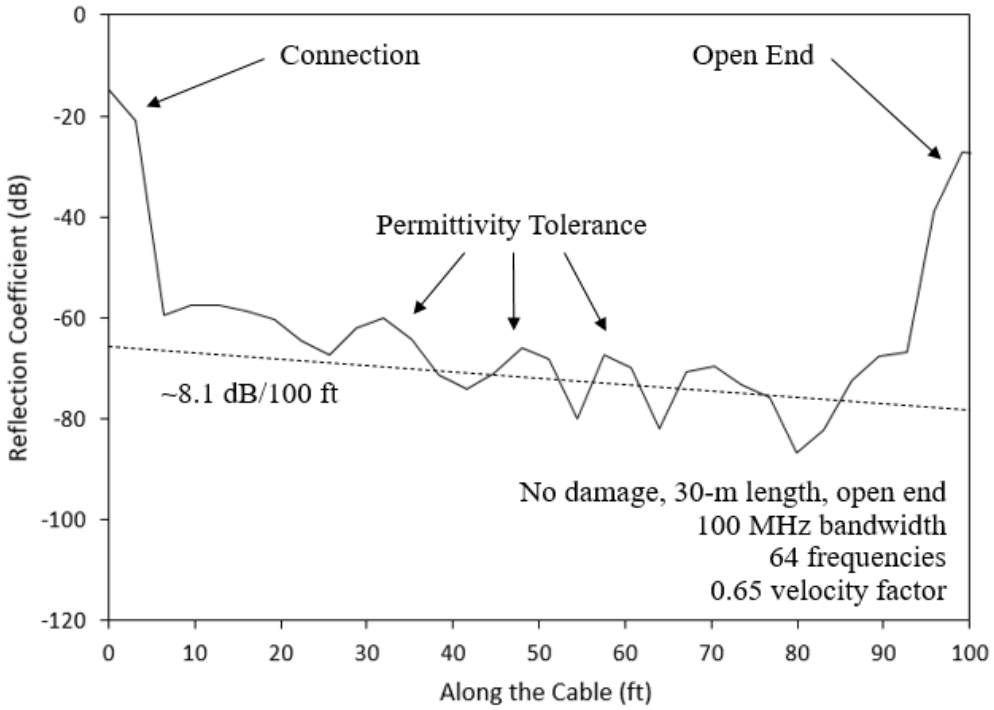

Figure 2-8. FDR response of the undamaged baseline electrical cable digital twin in the time domain.

2.3.2 Calibrating the Digital Twin

Development of an electrical cable digital twin is challenged by 1) accuracy and 2) simulation time. In terms of accuracy, improvements can be made by increasing the density of the mesh (both cross-sectional and swept), increasing the evaluated bandwidth, and/or improving the connection impedance or permittivity variance. An improvement or reduction in simulation time can be found by reducing the density of the mesh, decreasing the bandwidth, and/or reducing the number of evaluated frequencies. However, trade-offs are typically found between accuracy and simulation time as observed when increasing or decreasing the mesh density. Therefore, it is important to evaluate the effect of various inputs on the digital twin to calibrate and optimize its response.

2.3.2.1 *Effect of Bandwidth*

Bandwidth is defined as the frequency range over which the simulation is conducted. The effect of bandwidth on the baseline digital twin response (at 256 frequencies) is shown in Figure 2-9 for bandwidths of 50, 100, 200, and 300 MHz. As shown in the figure, increasing the bandwidth improved the resolution of the time domain response, in agreement with previous work (Glass et al. 2022) (spatial resolution of 6.4, 3.2, 1.6, and 1.1 ft found at bandwidths of 50, 100, 200, and 300 MHz, respectively). Within expectations, increasing the bandwidth was also observed to increase attenuation or equivalently to reduce the propagation length (1630, 815, 408, and 272 ft propagation length for bandwidths of 50, 100, 200, and 300 MHz, respectively). Since the signal must propagate down the length of the cable and back, and due to correlation of bandwidth with propagation length and consequently number of frequencies, a bandwidth of 100 MHz was selected for the baseline digital twin to optimize both spatial resolution and simulation time.

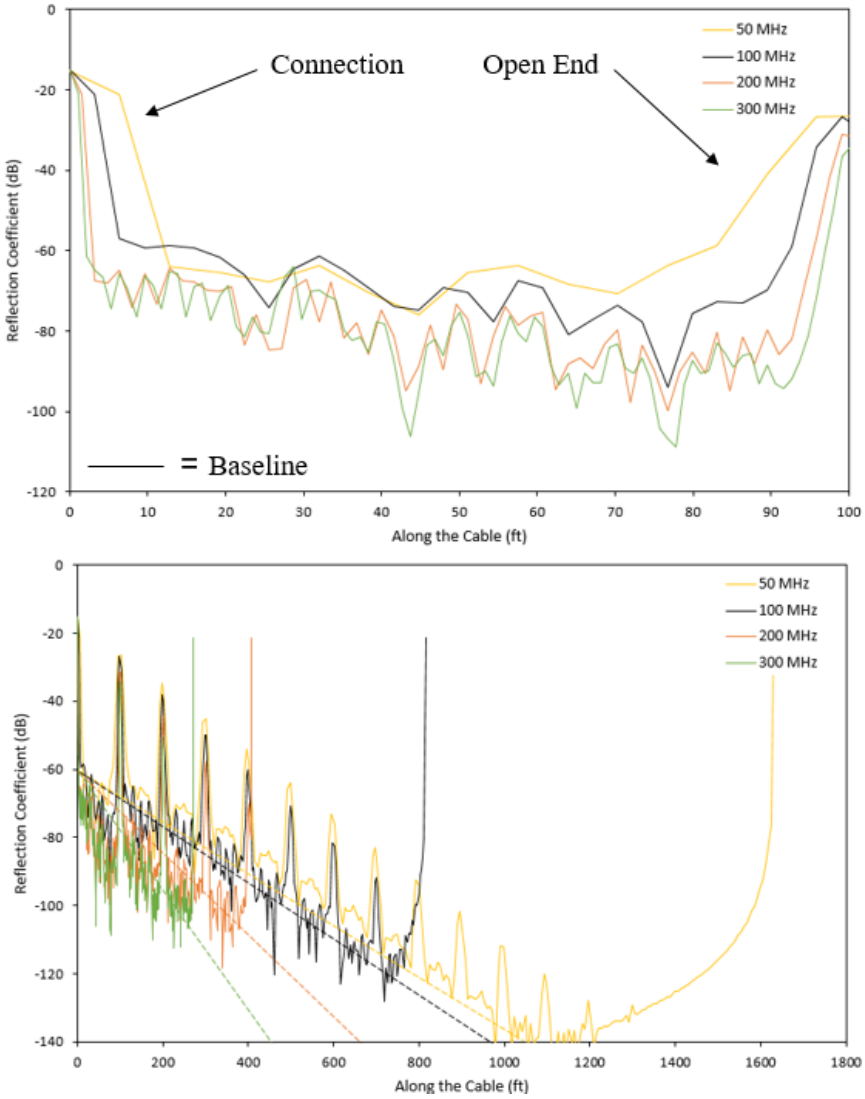

Figure 2-9. Effect of bandwidth on the electrical cable digital twin response demonstrating (top) spatial resolution and (bottom) propagated length and line loss. Baseline refers to the response of the baseline digital twin as discussed in Section 2.3.1.4.

2.3.2.2 *Effect of Number of Frequencies*

The number of frequencies is defined as the number of independent simulations carried out in sequence as discussed in Section 2.3.1.4; the number of frequencies is equivalent to the number of frequency samples specified for VNA measurement. The effect of the number of evaluated frequencies on the baseline digital twin response is shown in Figure 2-10 for 64, 128, and 256 frequencies. Similar to that observed in previous work (Glass et al. 2021), increasing the number of evaluated frequencies increased the propagation length of the signal. Furthermore, at least 64 frequencies were required to ensure that the signal propagated to the end of the cable and back again (approximately 201 ft propagation at 100 MHz bandwidth). In terms of simulation time, approximately 20, 40, and 60 minutes were required to solve the simulation for 64, 128, and 256 frequencies, respectively. Lastly, convergence was found for the time domain response with at least 128 evaluated frequencies; however, in this work it was observed that 64 frequencies provided adequate accuracy to evaluate defects and therefore the baseline digital twin incorporated 64 frequencies to reduce simulation time.

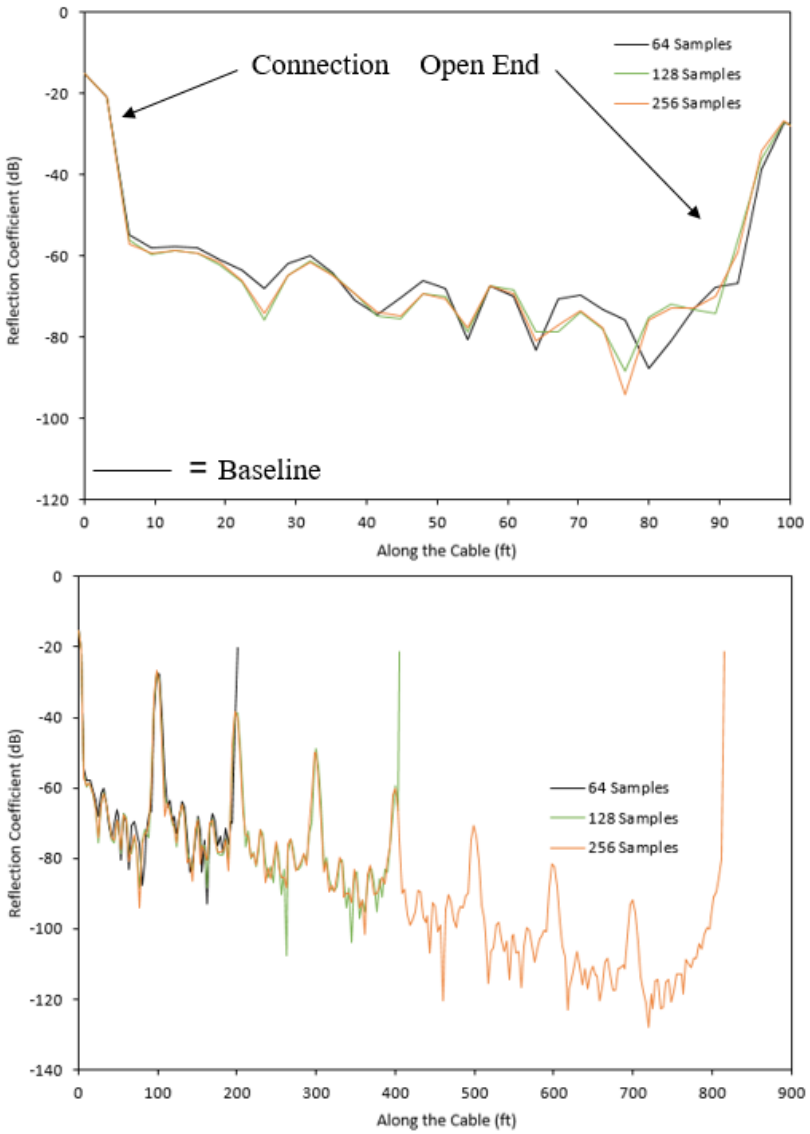

Figure 2-10. Effect of number of frequencies on the electrical cable digital twin response showing (top) convergence and (bottom) propagated length. Baseline refers to the response of the baseline digital twin as discussed in Section 2.3.1.4.

2.3.2.3 Effect of Port Impedance

Port impedance is defined as the characteristic impedance specified at the lumped port (see Section 2.3.1.2). The effect of port impedance on the baseline digital twin response is shown in Figure 2-11 for impedances of 50, 500, 5000, and 50000 Ω. With increasing port impedance, increasing port loss was observed (approximately 39, 41, 55, and 63 dB port loss for 50, 500, 5000, and 50000 Ω port impedance, respectively). Furthermore, increasing the port impedance was found to diminish the response from permittivity variance. For the baseline digital twin, a connection impedance of 50 Ω was selected to minimize port loss and the effect on permittivity variance. Future work could focus on improving the response of the electrical cable digital twin at the location of the port, particularly towards reducing port loss (< 30 dB).

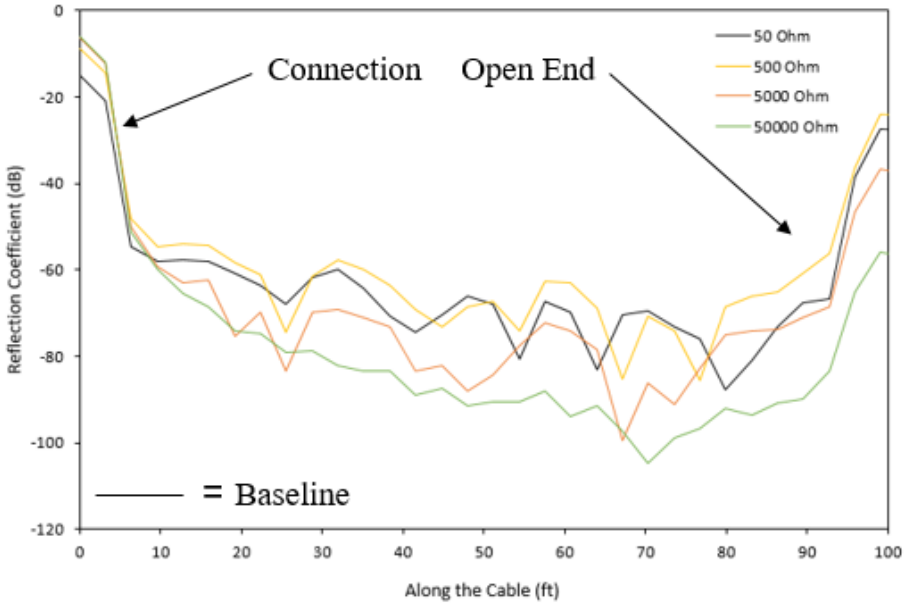

Figure 2-11. Effect of connection impedance on the electrical cable digital twin response. Baseline refers to the response of the baseline digital twin as discussed in Section 2.3.1.4.

2.3.2.4 Effect of Permittivity Variance

Permittivity variance is defined as small Gaussian permittivity variations applied to each of the 30 segments in the digital twin to produce random variations in the time domain response. The effect of permittivity variance on the baseline digital twin response is shown in Figure 2-12 for standard deviations of 0.005, 0.010, 0.015, and 0.020 with a mean of 0.0. As expected, increasing the standard deviation produced increased variations (ΔdB) or "noise" within the time domain response of the digital twin; more specifically, ΔdB was found to be 12, 18, 21, and 26 dB when measured from 20-to-80 ft for standard deviations of 0.005, 0.010, 0.015, and 0.020, respectively. For comparison to previous work, the baseline digital twin incorporated a modified 0.010 standard deviation.

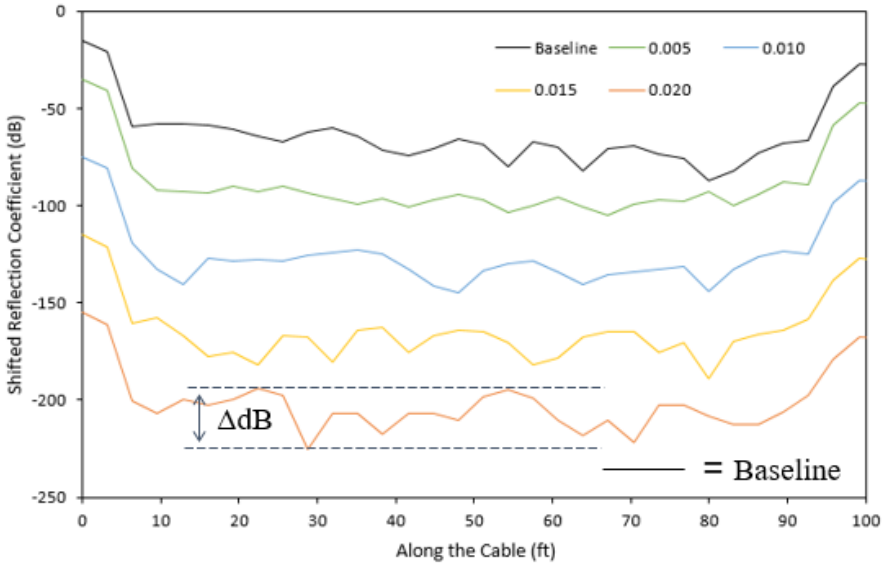

Figure 2-12. Effect of permittivity variance on the electrical cable digital twin response. Baseline refers to the response of the baseline digital twin as discussed in Section 2.3.1.4.

2.3.2.5 Effect of Cross-sectional Mesh

The effect of cross-sectional mesh on the baseline digital twin response is shown in Figure 2-15 for coarse, medium (actual mesh that was used), and fine mesh. First, with increasing number of elements, a corresponding increase in nodal locations and therefore degrees of freedom are found. As solution time is proportional to the square of the degrees of freedom, increasing the number of elements has a significant impact on simulation time as shown in Figure 2-13. Next, evaluation of the quality of mesh is commonly conducted using attributes such as skewness or maximum angle. In this work, mesh was evaluated by calculating the magnitude of mesh quality for skewness, maximum angle, volume versus length, and growth rate, see Figure 2-14. As such, mesh quality has an upper bound of 2.0, which represents a perfectly regular element. With reduced mesh quality, convergence and consequently stability of the digital twin can be impacted. Overall, mesh quality was found to be similar for both the medium and fine mesh. Finally, it is of critical importance to ensure convergence of results with increasing mesh density. As shown in Figure 2-15, approximate results were found for all three evaluated mesh densities; however, the medium mesh was selected to ensure a mesh quality of at least 1.20 or higher.

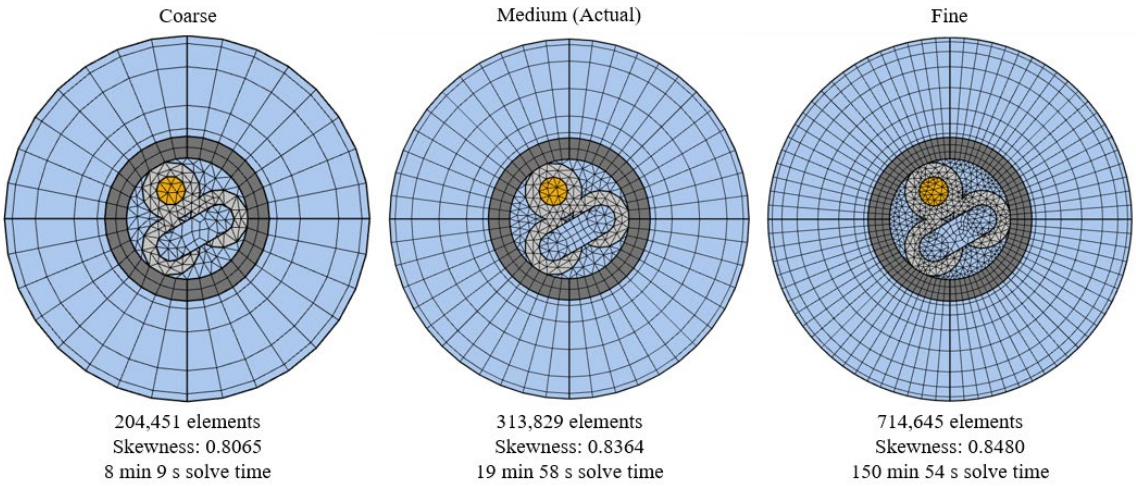

Figure 2-13. Evaluated cross-sectional mesh for electrical cable digital twin.

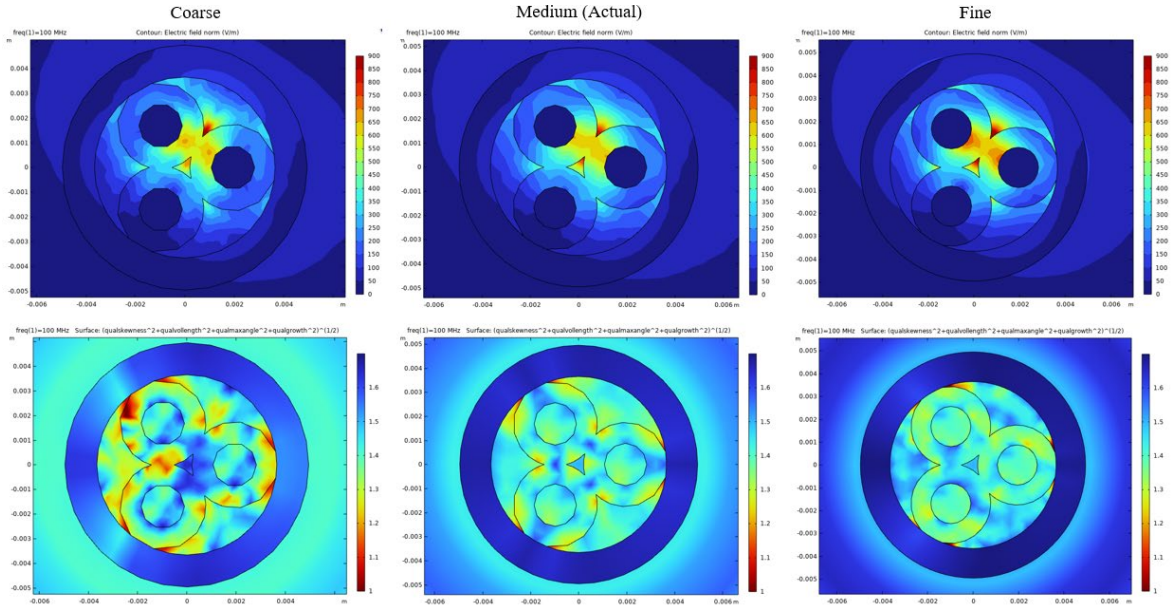

Figure 2-14. (Top) electric field and (bottom) overall mesh quality for evaluated cross-sectional mesh densities.

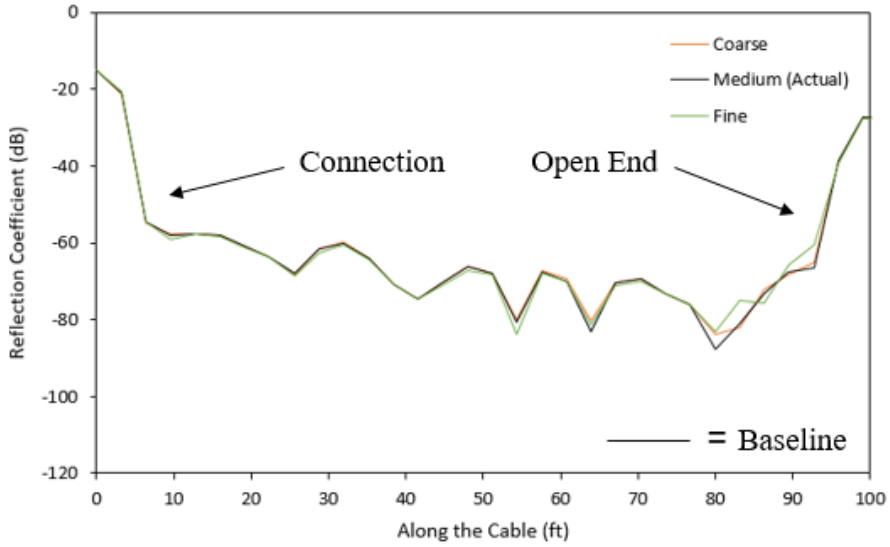

Figure 2-15. Effect of cross-sectional mesh on the electrical cable digital twin response. Baseline refers to the response of the baseline digital twin as discussed in Section 2.3.1.4.

2.3.2.6 Effect of Swept Mesh

Swept mesh length is defined as the amount of discretization along the length of the cable for each segment. The effect of swept mesh length on the baseline digital twin response is shown in Figure 2-16 for swept mesh lengths λ/10, λ/20, or λ/30 where λ is the minimum wavelength. With decreasing swept lengths, the total number of elements increases and consequently simulation time increases (solution times of 7, 20, and 40 minutes with swept lengths of λ/10, λ/20, and λ/30, respectively). Furthermore, lengthening the swept elements also increases the skewness of the elements (0.826, 0.836, 0.841 skewness quality for swept lengths of λ/10, λ/20, and λ/30, respectively). Lastly, with a swept length of λ/10, velocity of propagation and end response variations were observed. Therefore, a swept mesh length of λ/20 was selected for the baseline digital twin to balance accuracy with a manageable simulation time.

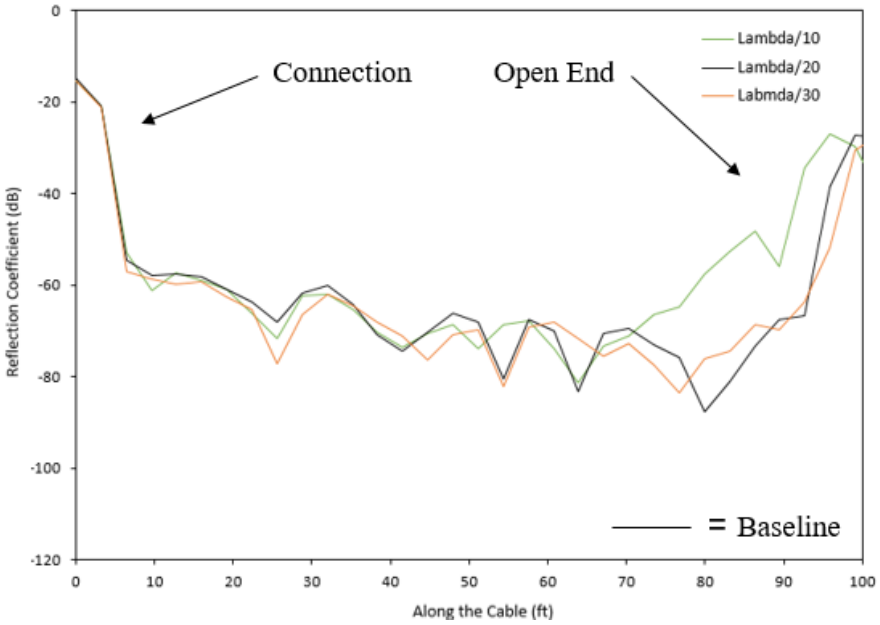

Figure 2-16. Effect of swept mesh on the electrical cable digital twin response. Baseline refers to the response of the baseline digital twin as discussed in Section 2.3.1.4.

3. RESULTS AND DISCUSSION

In this section, the electrical cable digital twin was evaluated for response to different test scenarios or anomalies, including comparison to physical ARENA test data. In addition, the digital twin was extended to approximately 1000 ft to demonstrate application of the digital twin to realistic cable lengths, including the effect of anomalies.

3.1 Evaluation of the Digital Twin

The electrical cable digital twin was evaluated to determine if commonly occurring electrical cable anomalies can be detected. Such anomalies could include damage to the insulation, routing of the cable through a water bath or oven, or a combination of damage types. Furthermore, the digital twin was evaluated to determine the effect of spectral permittivity on its response. All comparisons are made to an undamaged cable (the baseline response defined in Figure 2-8) and using reflection coefficient magnitude (given in arbitrary units, a.u.), as opposed as decibels, to enhance comparison.

3.1.1 Effect of Anomaly Type

To evaluate the digital twin on its response to anomalies, the following anomalies were investigated:

A. Insulation Damage (Section 3.1.1.1)
B. Water Bath (Section 3.1.1.2)
C. Moisture Ingress (Section 3.1.1.3)
D. Thermal Aging (Section 3.1.1.4)
E. Combination Damage (Section 3.1.1.5)

3.1.1.1 *Insulation Damage*

The effect of local insulation damage on the electrical cable digital twin response is shown in Figure 3-1 and Figure 3-2 for insulation permittivity of 120% from 26.2-to-29.5 ft and 36.1-to-59.1 ft, respectively; prior work has shown insulation witness samples of thermally damaged electrical cables to have an insulation permittivity increase of 20% or more relative to the undamaged value (Fabiani et al. 2018). As expected from previous work (Glass et al. 2017), an increase in the reflection coefficient was observed at the location of the single defect at approximately 28 ft; here, a single defect was observed due to the spatial resolution at 100 MHz (3.2 ft) being similar to the size of the anomaly (3.3 ft). Increasing the size of the defect produced two peaks, one for entrance into the defect region and one for exiting, again similar to prior work and within expectations (Glass et al. 2017). The reduction of the reflection coefficient peaks for damage from 36.1-to-59.1 ft compared to 26.2-to-29.5 ft was unexpected and potentially due to the incorporated permittivity variance or due to only incorporating the real portion of permittivity (not incorporating the imaginary portion of the permittivity). Lastly, the usage of a damage trace (damaged response subtracted from undamaged response) was observed to further improve detection of the anomaly.

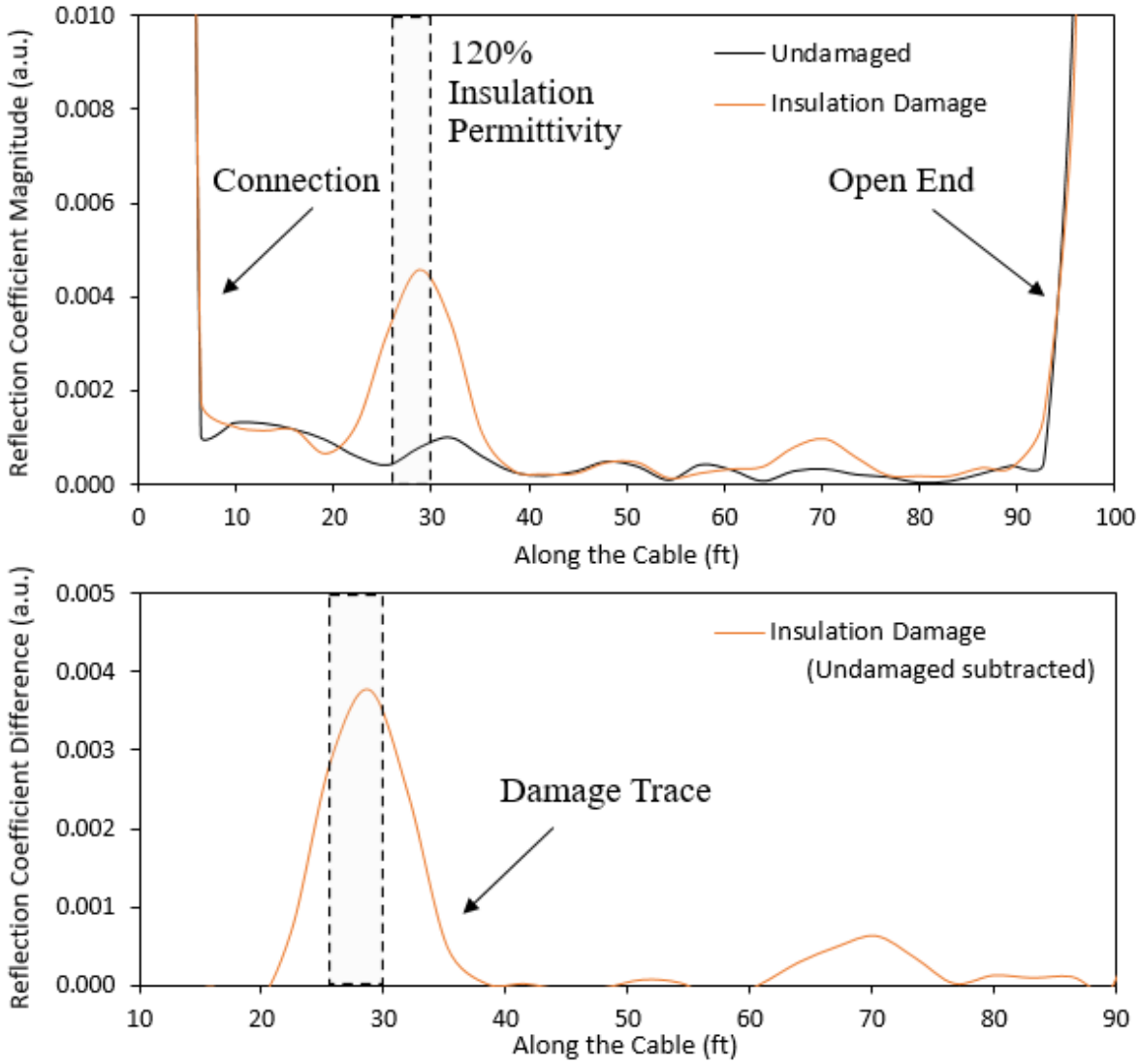

Figure 3-1. (Top) Effect of insulation permittivity on the digital twin response for a defect from 26.2-to-29.5 ft and (bottom) corresponding damage trace (undamaged subtracted from damaged response).

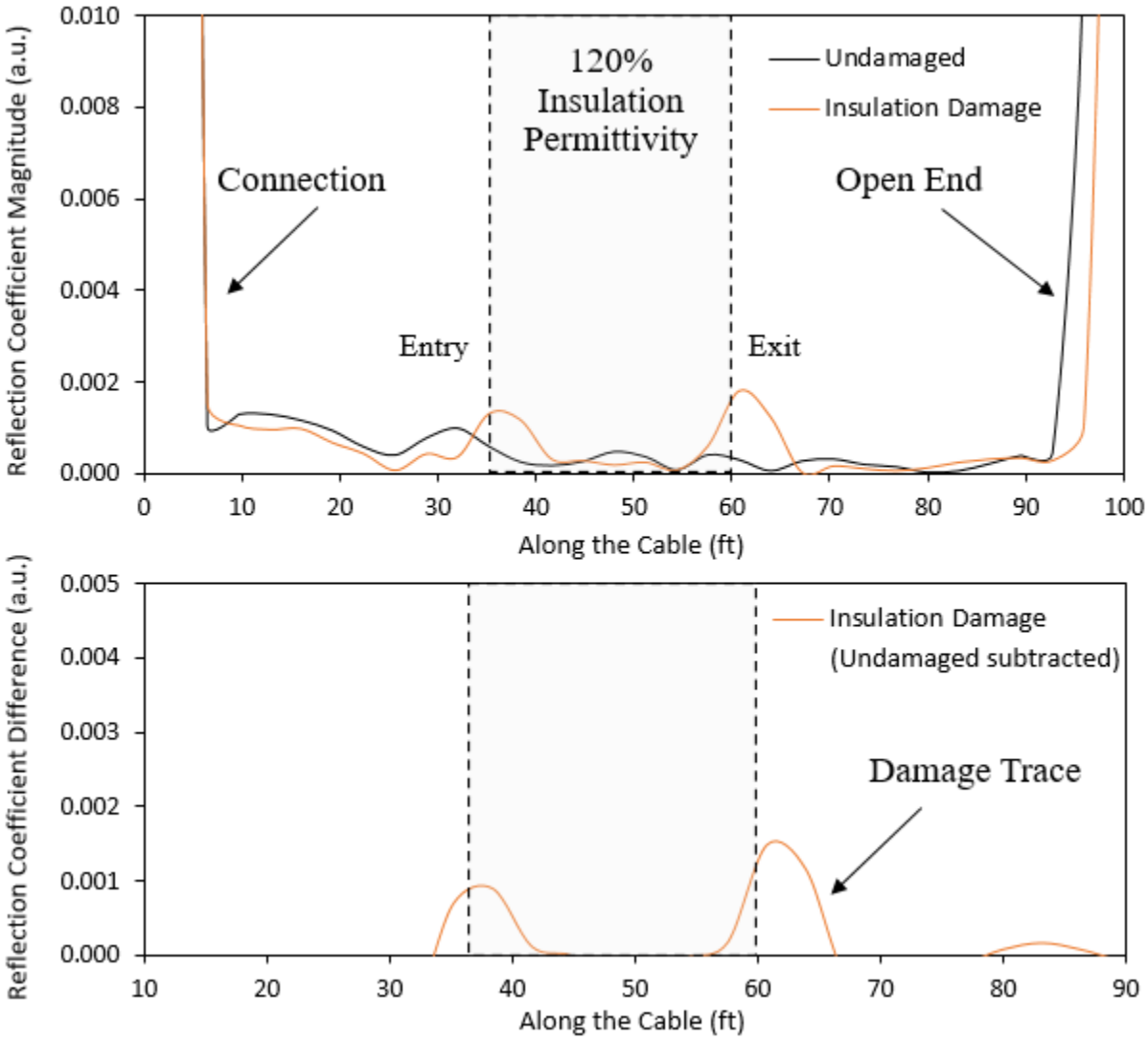

Figure 3-2. (Top) Effect of insulation permittivity on the electrical cable digital twin response for a defect from 36.1-to-59.1 ft and (bottom) corresponding damage trace (undamaged subtracted from damaged response).

3.1.1.2 Water Bath

The effect of a water bath on the electrical cable digital twin response is shown in Figure 3-3 for water surrounding the cable from 26.2-to-39.4 ft (assuming water relative permittivity of 80). As the baseline digital twin is a non-shielded electrical cable, detection of external water, such as by immersion in a water bath, was confirmed as expected based upon literature (Glass et al. 2021). In addition, minor velocity of propagation variations were found at the location of the water bath exit and at the open end, similar to that observed in previous work (Glass et al. 2021). Finally, the damage trace was observed to produce significant anomaly peaks at the location of the water bath entrance and exit.

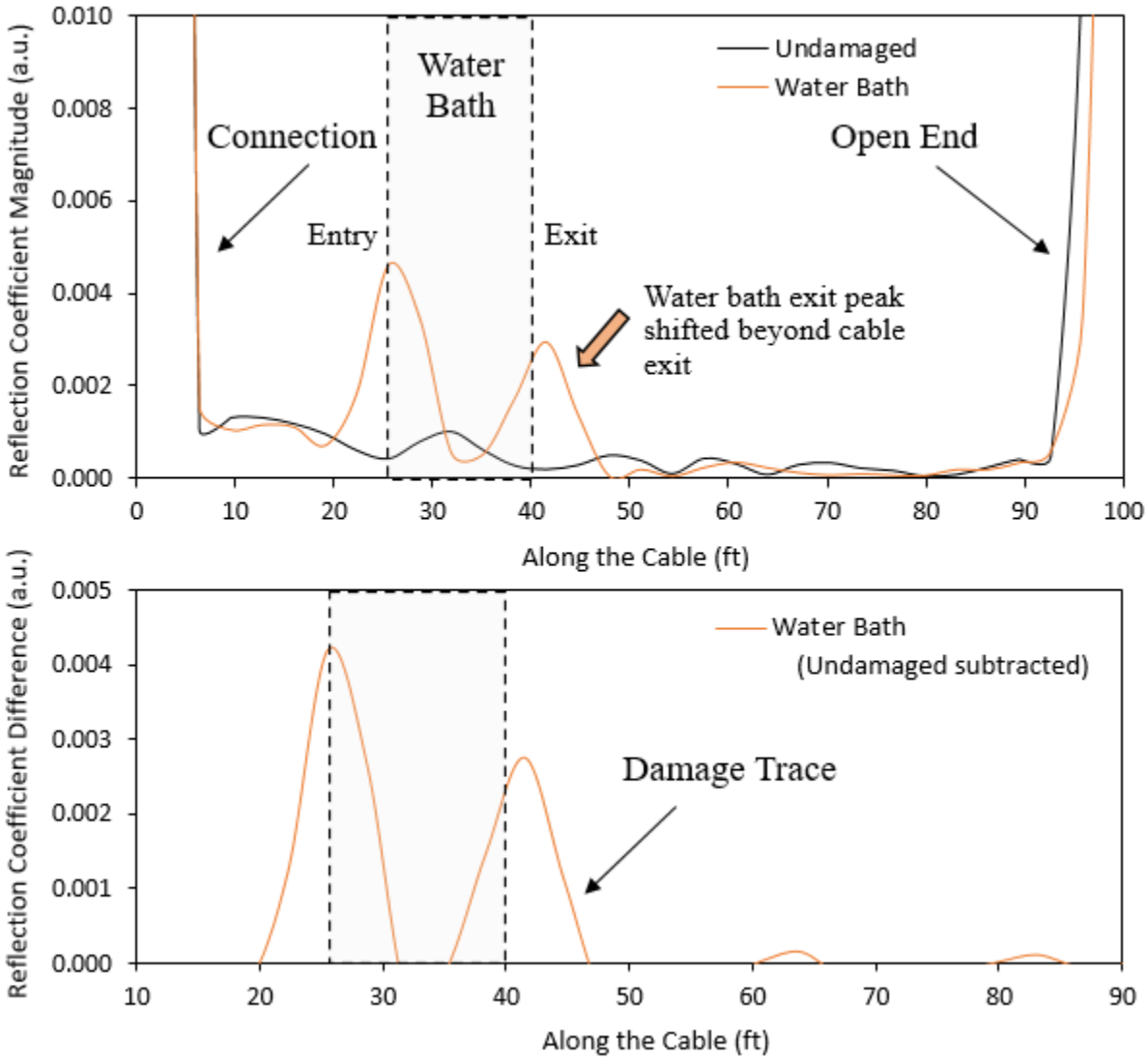

Figure 3-3. (Top) Effect of a water bath on the electrical cable digital twin response and (bottom) corresponding damage trace (undamaged subtracted from damaged response). Note that the shifted exit response due to velocity of propagation decrease is predicted.

3.1.1.3 *Moisture Ingress*

The effect of moisture ingress on the electrical cable digital twin response is shown in Figure 3-4. In this example, water was modeled as having ingressed from the open end of the cable up to 62.3 ft (as measured from the lumped port or connection). As expected, internal water was readily detectable with a large reflection coefficient peak forming at approximately 62.3 ft. Furthermore, moisture ingress was observed to have a significant impact on the velocity of propagation of the signal, in particular when compared to the effect of external water shown in Figure 3-3. The effect of moisture ingress was also observed to produce an increased damage trace response when compared to water surrounding the cable, again within expectations as the strength of the generated electric field is greater within the cable.

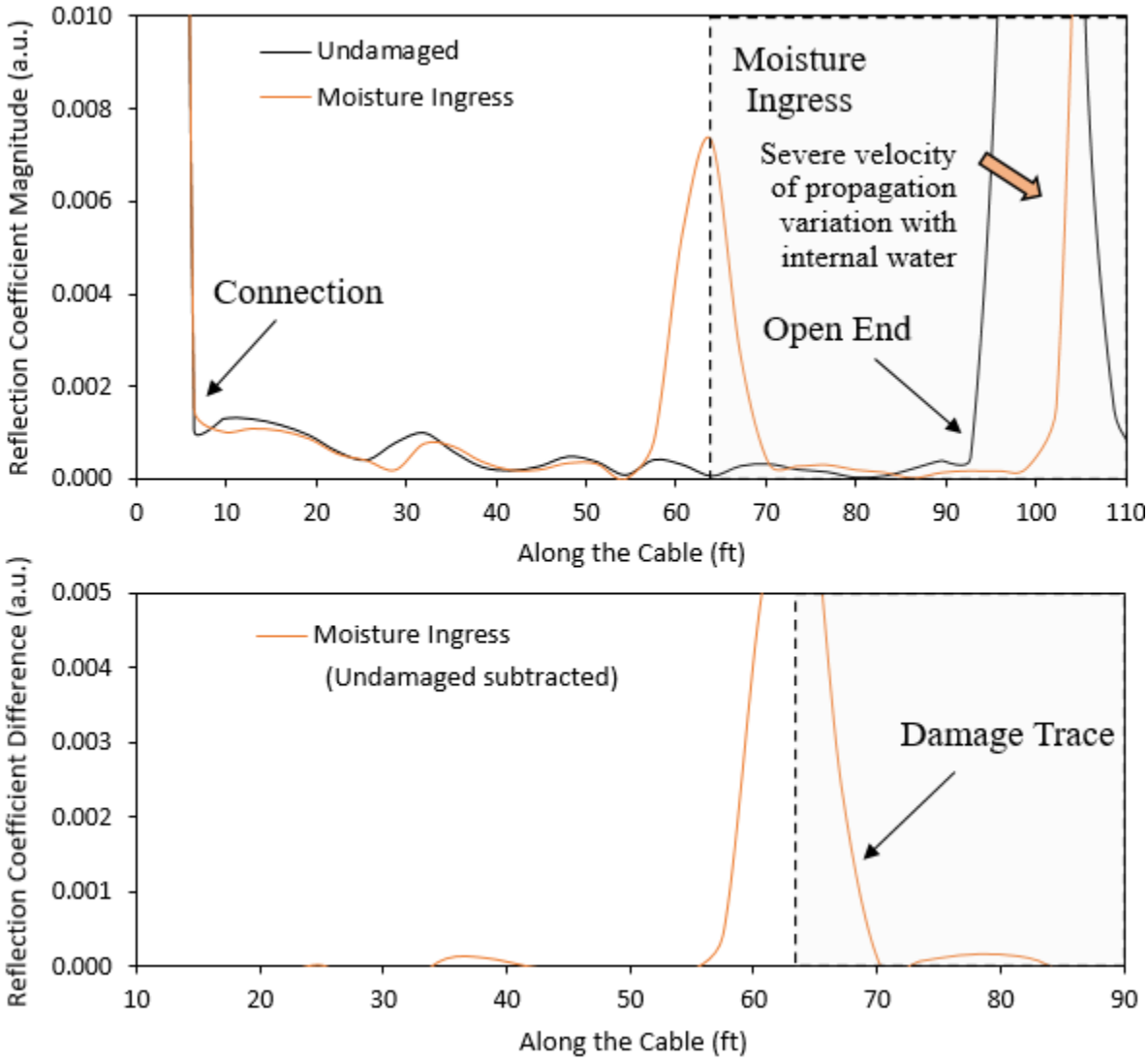

Figure 3-4. (Top) Effect of moisture ingress on the electrical cable digital twin response and (bottom) corresponding damage trace (undamaged subtracted from damaged response).

3.1.1.4 Thermal Aging

Thermal aging has been shown to increase insulation permittivity by up to 20% (Fabiani et al. 2018). The effect of thermal aging on the digital twin response is shown in Figure 3-5 for 100% (undamaged), 110%, and 120% insulation permittivity from 42.7-to-72.2 ft. Here, it was observed that increasing permittivity led to increasing reflection coefficient response over the aging region, similar to previous work (Glass et al. 2022). Furthermore, the usage of a damage trace produced clear aging trends.

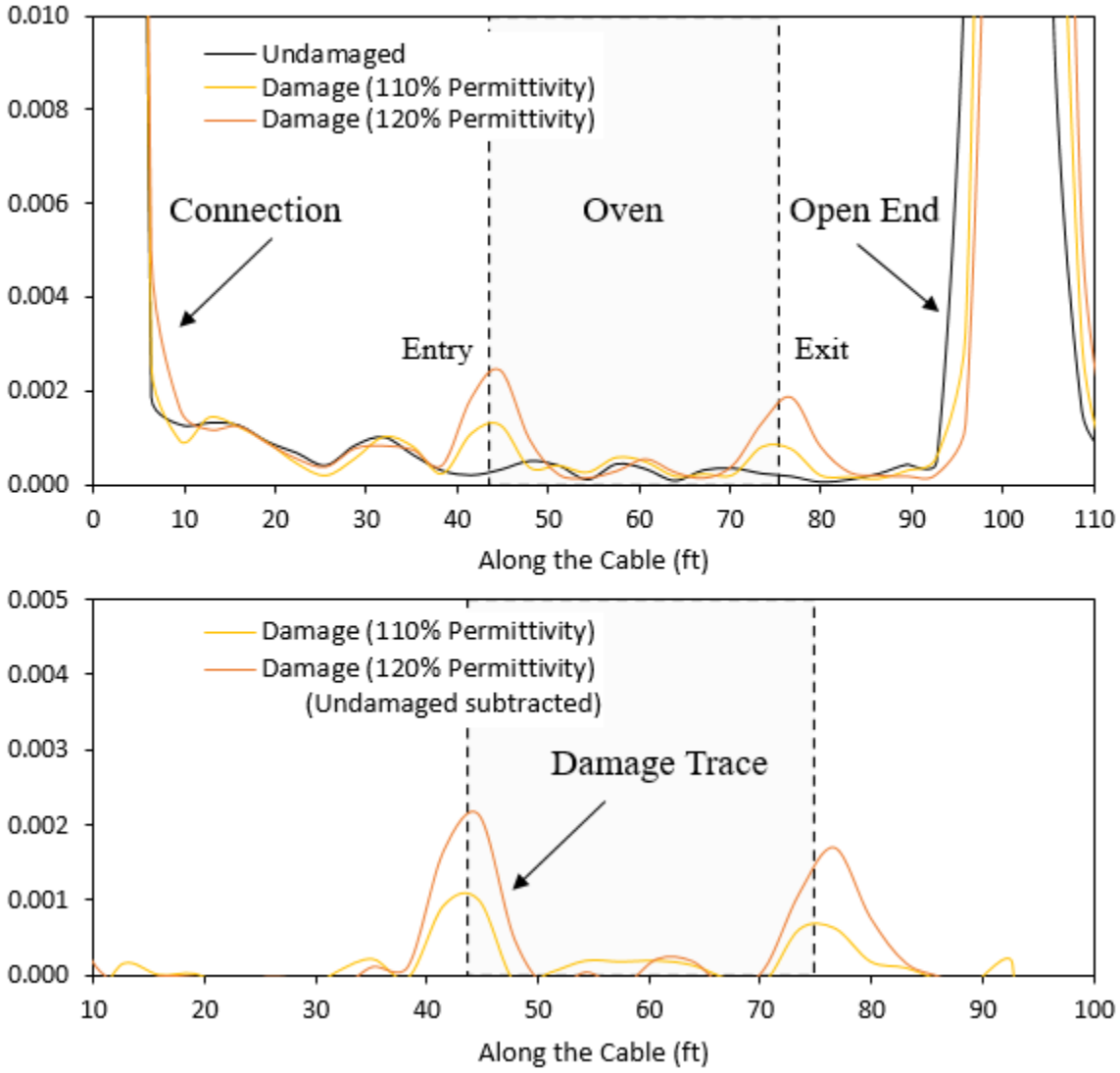

Figure 3-5. (Top) Effect of thermal aging on the electrical cable digital twin response and (bottom) corresponding damage trace (undamaged subtracted from damaged response).

3.1.1.5 Combination Damage

The effect of combination damage, including a water bath, permittivity variation (e.g., oven), and moisture ingress, on the electrical cable digital twin response is shown in Figure 3-6. In this example, external water was located from 26.2-to-39.4 ft (a water bath), 120% insulation permittivity from 45.9-to-65.6 ft (an oven), and internal water from 75.5-to-78.7 ft (water ingress). As shown in the figure, all three anomalies were detectable with the digital twin, including velocity of propagation variations. As observed, an increased damage trace response was observed for external and internal water compared to the insulation damage.

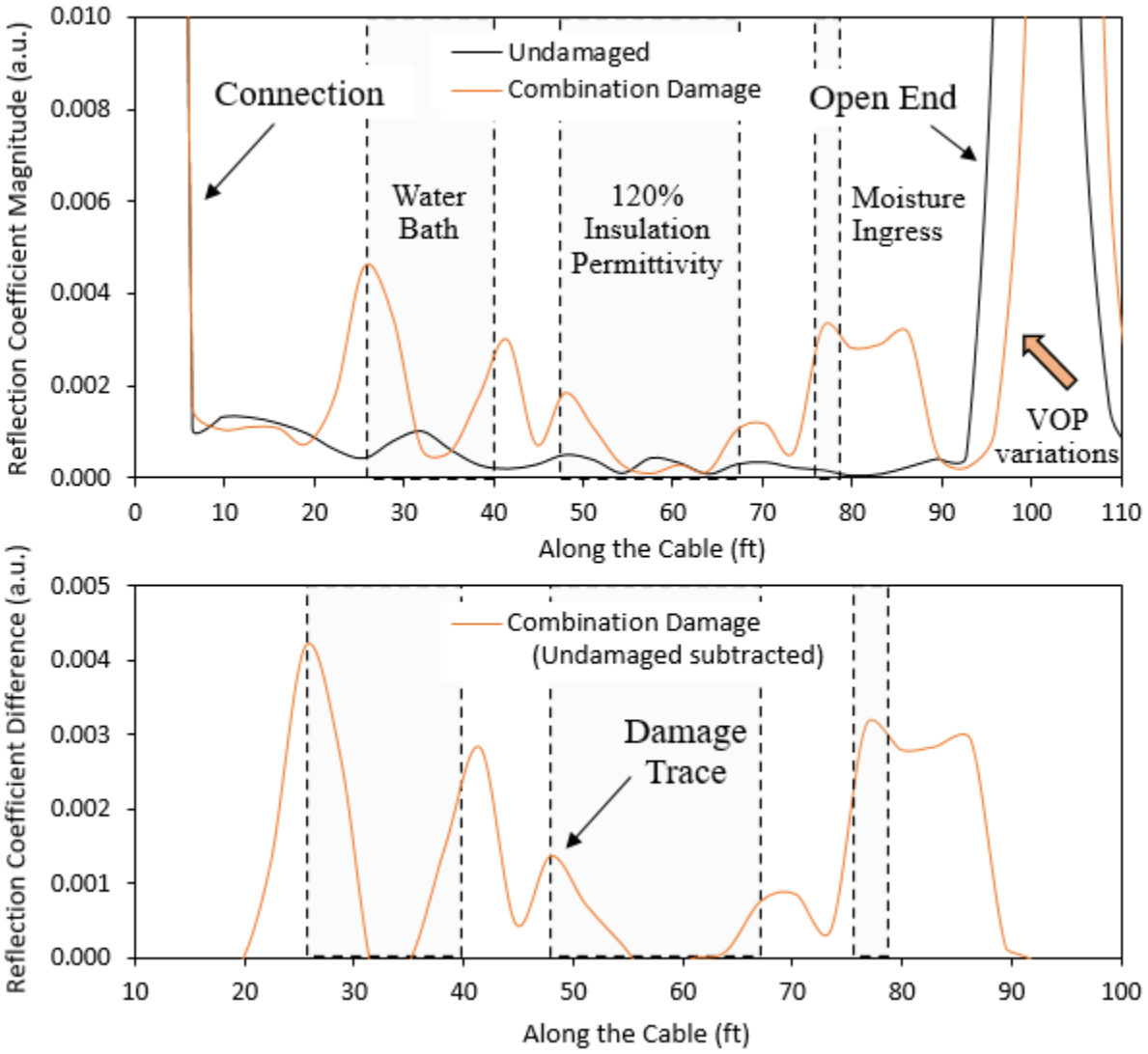

Figure 3-6. (Top) Effect of combination damage (water bath, insulation permittivity, and moisture ingress) on the electrical cable digital twin response and (bottom) corresponding damage trace (undamaged subtracted from damaged response).

3.1.2 Effect of Spectral Permittivity

The effect of spectral insulation permittivity on the electrical cable digital twin response is shown in Figure 3-7 for 120% insulation permittivity variation from 42.7-to-72.2 ft. As discussed in Section 2.3.1.1, the baseline digital twin incorporates spectral permittivity for the insulation of the form,

$$\varepsilon(f) = -1.3631 \cdot 10^{-10} f + 2.72.$$

To evaluate and compare the effect of spectral permittivity, simulations were conducted with the above spectral permittivity and with a constant global insulation permittivity of 2.72. With either spectral or constant permittivity for the insulation, damage peaks were identifiable and similar in magnitude. Furthermore, end responses were observed to be comparable with and without spectral content, with no velocity of propagation variation found.

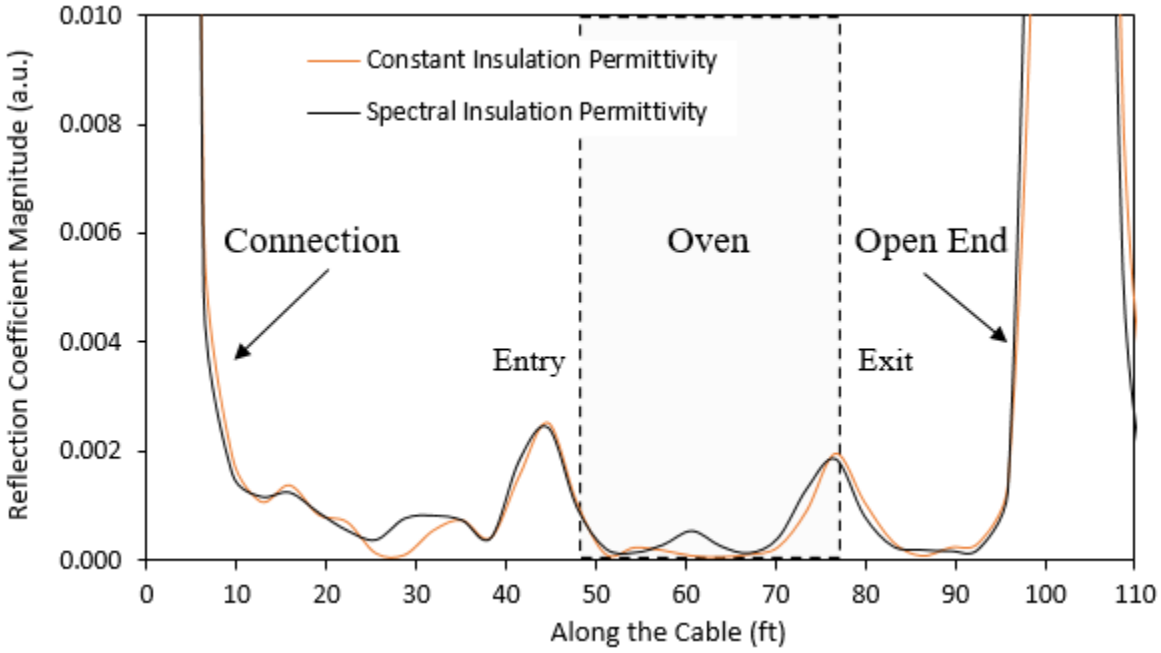

Figure 3-7. Effect of spectral permittivity on the electrical cable digital twin response for a simulated thermal oven.

3.2 Comparison to Test Data

To further confirm and validate the response of the electrical cable digital twin, comparisons were made to physical ARENA test data for the same cable undergoing thermal aging at 140°C for up to 62 days. As discussed in Section 2.2.3, spectral permittivity for the insulation was extracted from literature for comparison. As such, insulation permittivity for the digital twin was updated to the permittivity shown in Figure 2-3. Specifically, insulation permittivity from approximately 42.7-to-72.2 ft was specified as:

1) 0-days: $\varepsilon(f) = -5 \cdot 10^{-10} f + 2.77$,
2) 49-days: $\varepsilon(f) = -5 \cdot 10^{-10} f + 2.84$,
3) 70-days: $\varepsilon(f) = -7 \cdot 10^{-10} f + 2.91$,

Thus, aging was induced in the digital twin from approximately 42.7-to-72.2 ft by incorporating the aged spectral permittivity. Furthermore, the global (non-aged or non-damaged) insulation permittivity was set to the 0-day spectral permittivity specified above. Note that aging for the experimental results occurred from approximately 45-to-75 ft as discussed in Section 2.2.1.

Results for aging time points of 0, 49, and 70 days for the digital twin and 0, 49, and 62 days for ARENA experimental results are shown in Figure 3-8. Here, the random coefficients for the digital twin insulation permittivity were removed to facilitate comparison; the effect on the 0 day or unaged digital twin response is significant as shown in the figure. First, velocity of propagation variations were observed only with experimental data, potentially due to differences in the aged permittivity of the actual insulation versus literature values incorporated. Furthermore, spectral permittivity incorporated in the digital twin included only the real component of permittivity – potential improvements in velocity of propagation may be obtained by including the imaginary component of permittivity as well. However, note that velocity of propagation variations were observed in the digital twin response with increased permittivity as shown in Figure 3-5 or with water as shown in Figure 3-3 and Figure 3-4. Second, due to differences in port loss between experimental measurements and the digital twin, an offset of approximately 20 dB was found between time domain results; reduction of the digital twin port loss could potentially be resolved by improving the method of signal injection (e.g., the lumped port). Third, oven entry and exit peaks were observed within both experimental and digital twin results. Fourth, increasing peak heights were observed with increasing aging time for both experimental and digital twin data at the oven entry and exit (e.g., 49 versus 62 days). Lastly, direct comparisons were made between oven entry and exit peaks, see Figure 3-9; oven entry and exit trends were found to be similar between the data sets, with less loss at the oven exit for the digital twin compared to experimental.

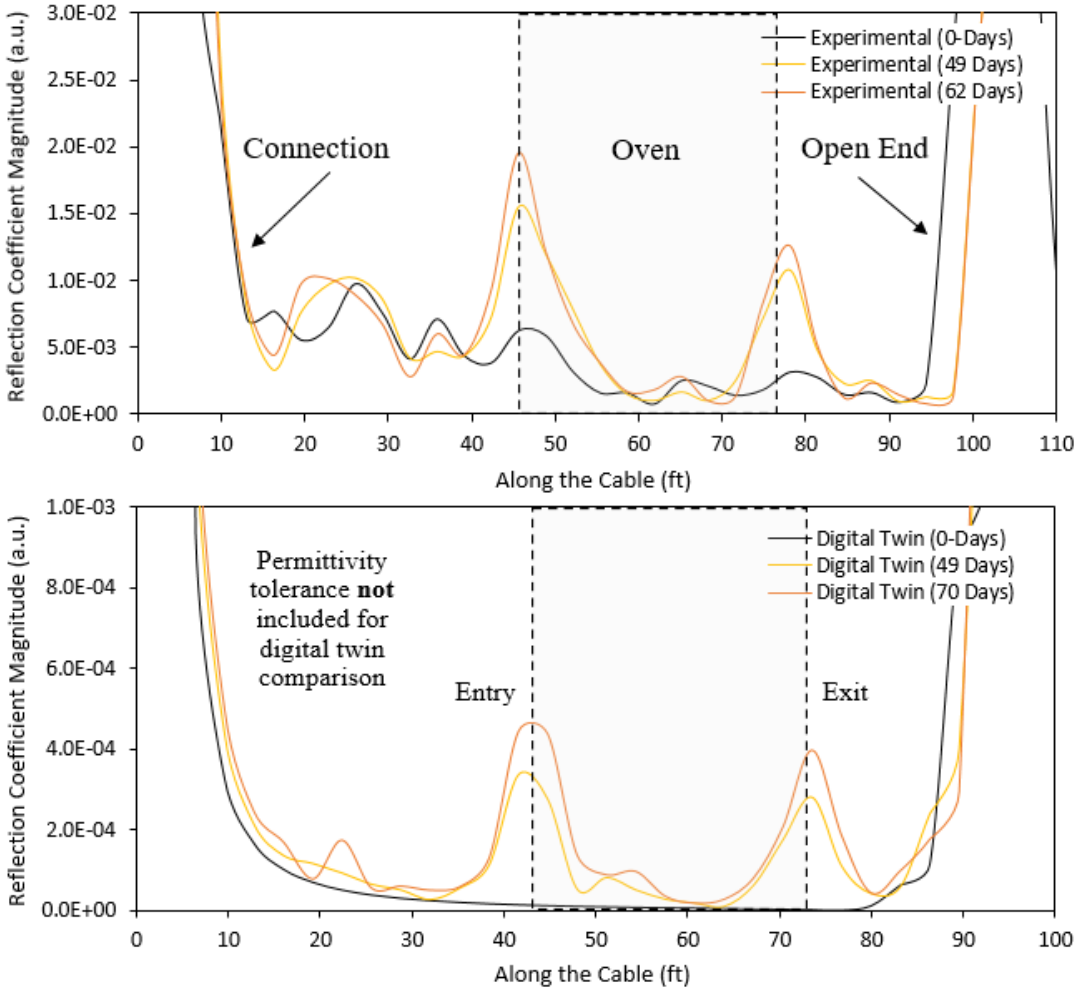

Figure 3-8. Comparison of (top) ARENA test data to the (bottom) digital twin at aged time points with oven entry and exit peaks indicated. To improve comparison, the digital twin results do not include permittivity variance which is especially noticeable for the 0-day results.

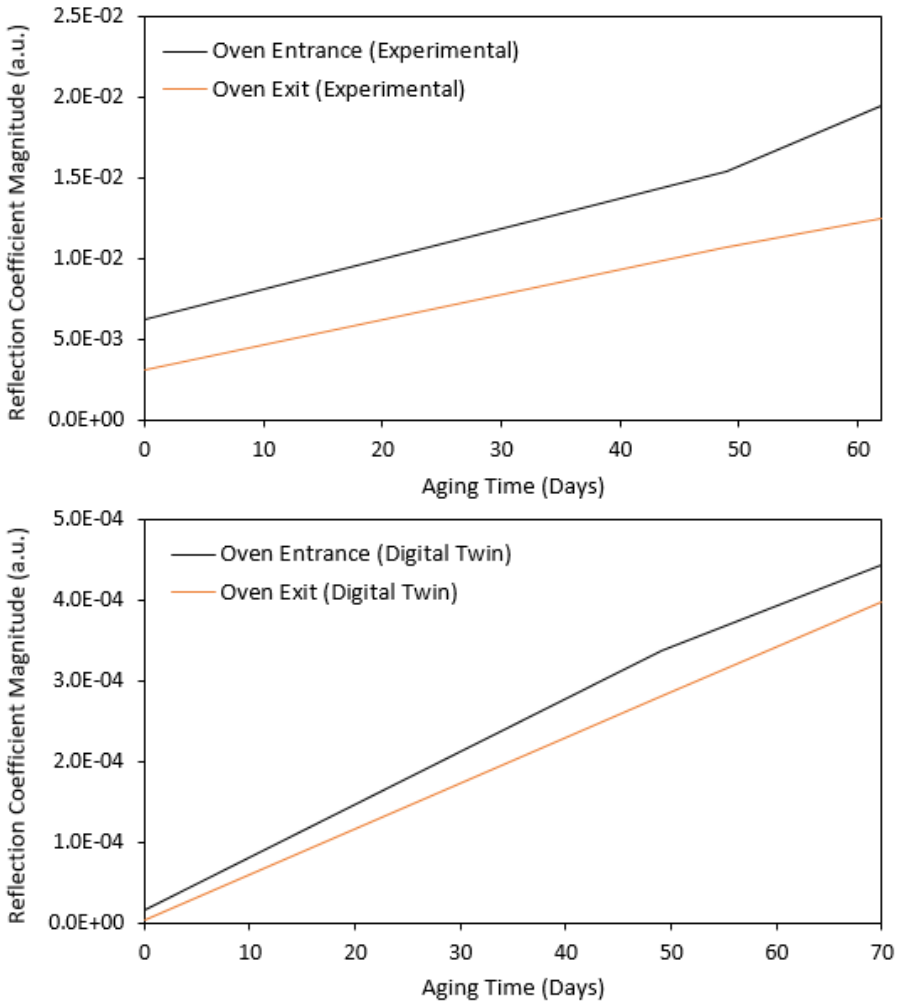

Figure 3-9. Comparison of oven entrance and exit trends for experimental and digital twin data.

3.3 Extension to 1000 ft Length

As a final confirmation of the electrical cable digital twin response, the length of the digital twin was extended from approximately 100 ft to 1000 ft to mimic actual in-service NPP electrical cables. To extend the digital twin to 1000 ft, the bandwidth was decreased to 75 MHz (100 to 175 MHz) and 512 uniformly spaced frequencies were evaluated; this increased the propagation length of the signal to approximately 2178 ft, which was greater than twice the approximately 1000 ft selected length of the cable. In addition, the reduced bandwidth produced a spatial resolution of 4.3 ft. To better resolve variations in the signal over 1000 ft, the digital twin was partitioned into 60 segments as opposed to the 30 segments incorporated for a length of 100 ft; therefore, each segment represented 16.4 ft of the electrical cable. Permittivity variance was specified for each segment at a standard deviation of 0.005, which was less than the 0.01 standard deviation specified for the baseline digital twin to improve visualization of defects. To reduce the solution time, the mesh was selected to be coarser than the coarse mesh indicted in Figure 2-13; more specifically, a swept mesh length of $\lambda/15$ produced nearly 900,000 elements with a solution time of 200 min.

The response of the digital twin at 1000 ft length is shown in Figure 3-10. Three defects were included:

a) 110% insulation permittivity from 115-to-131 ft (one segment),
b) 110%, 130%, 120%, and 110% permittivity in sequence from 328-to-394 ft (four segments),
c) 120% insulation permittivity from 705-to-722 ft (one segment).

All three defects were clearly observed in the digital twin response. Both single segment defects (a and c) demonstrated two peaks due to the size of the segments (16.4 ft) compared to the spatial resolution at the evaluated bandwidth (4.3 ft), a phenomenon that has previously been observed (Glass et al. 2017). Furthermore, a larger response was observed with 120% insulation permittivity from 705-to-722 ft compared to 110% insulation permittivity form 115-to-131 ft, within expectations. The four damaged segments from 328-to-394 ft appear to have an increased response at the 130% insulation permittivity compared to the other adjacent segments, also within expectations.

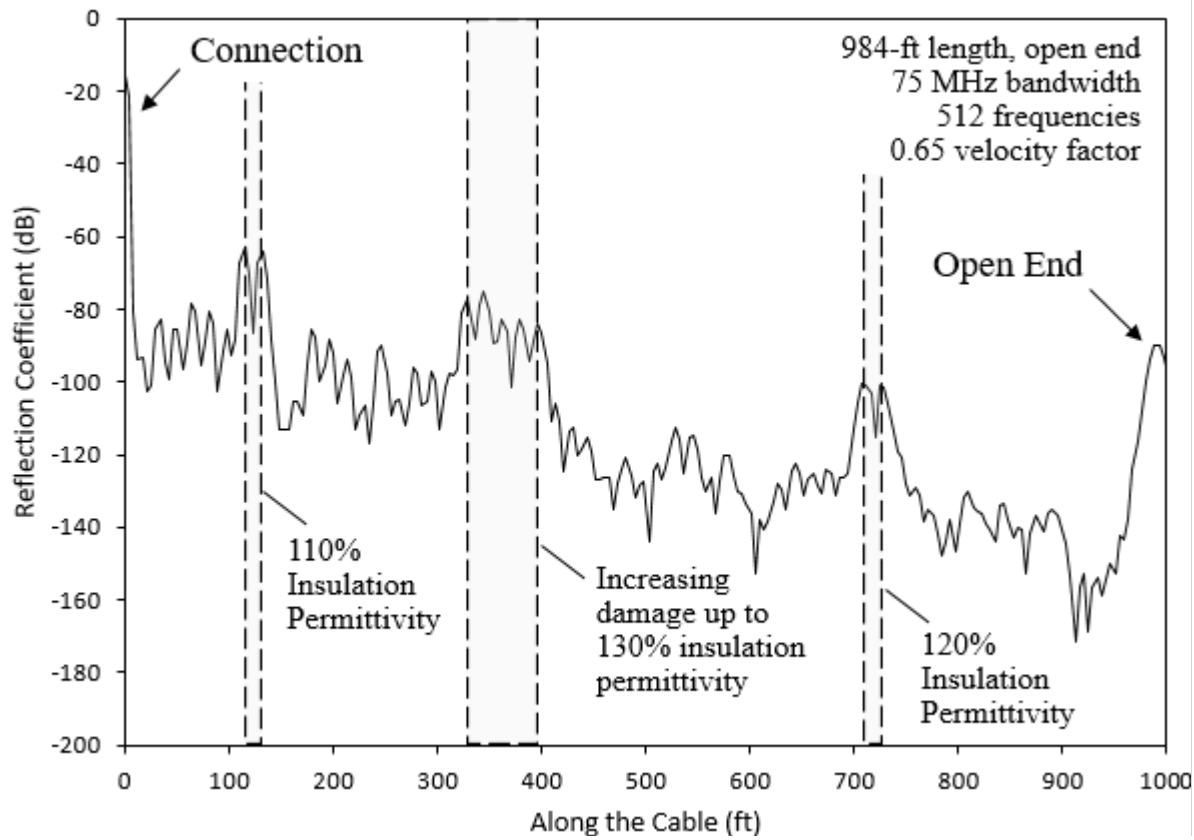

Figure 3-10. Extension of the electrical cable digital twin to 1000 ft. Defects were included from 115-to-131 ft, 328-to-394 ft, and 705-to-722 ft.

4. CONCLUSIONS

The objective of this work was to evaluate and confirm the response of a 3D FDR electrical cable digital twin. As a first step, the digital twin was developed towards the first level of achievement, namely demonstrating that the digital twin can be connected to the physical world. Observations and conclusions of this work include:

1. Fully 3D digital twin simulation of an electrical cable using an FDR approach is possible, but there are tradeoffs between simulation fidelity and solution time that must be balanced to ensure the simulation solves in a practical period of time (e.g., less than 20 minutes). Simulation parameters to balance include frequency bandwidth, number of frequencies, mesh density, connection impedance, and permittivity variance.

2. The digital twin simulation can explain FDR sensitivity to various cable anomalies, including entry and exit from an oven or water bath.

3. The digital twin simulation FDR response attenuates with distance along the cable and is further affected by the frequency bandwidth, similar to the response observed with physical measurements.

4. The resolution of the digital twin FDR peaks increases with increasing bandwidth and with increasing number of frequencies, again similar to physical measurements.

5. Display choices make a difference in the appearance of data signals and the ability of an analyst to detect anomalies. Display possibilities include dB attenuation from a normalized cable connection or end reflection reference, an absolute representation of the reflection coefficient, or a difference plot whereby the reference baseline is subtracted from the damaged cable response.

6. The presence of multiple anomalies in the digital twin does not substantially attenuate the FDR response to anomalies located beyond the first encountered anomaly and impedance mismatch.

7. Spectral variation of the permittivity does not have a significant effect on the FDR response compared to a fixed nominal permittivity value.

8. Extension of the digital twin to 1000 ft still allows for detection of distal anomalies near the far end of the electrical cable from the instrument connection point.

9. The ARENA test bed facilitates efficient nondestructive evaluation of well understood cable anomalies with various condition monitoring methods without risking actual plant system damage.

It is anticipated that electrical cable system digital twins, such as the one described here, will enable development of increasingly sophisticated and effective condition monitoring and prediction tools to support continued safe and efficient operation of light water reactors.

5. REFERENCES

Blocker, E., S. Smith, L. Philpot, and J. Conley. 1996. *Aging Management Guideline for Commercial Nuclear Power Plants - Electrical Cable and Terminations.* Sandia National Labs SAND96-0344, Albuquerque, NM. http://www.osti.gov/energycitations/product.biblio.jsp?osti_id=204243.

Fabiani, D., S. V. Suraci, and S. Bulzaga. 2018. "Aging Investigation of Low-Voltage Cable Insulation Used in Nuclear Power Plants." In *2018 IEEE Electrical Insulation Conference (EIC)*, 516–19. IEEE. https://doi.org/10.1109/EIC.2018.8481139.

Fifield, L. S., and R. Duckworth. 2015. "Progress in the Investigation Fo Nuclear Power Plant Cable Aging." In *17th International Conference on Environmental Degradation of Materials in Nuclear Power Systems -- Water Reactors* August 9-13, 2015, Ottowa, Ontario, Canada.

Furse, C., Y. C. Chung, R. Dangol, M. Nielsen, G. Mabey, and R. Woodward. 2003. "Frequency-Domain Reflectometery for on-Board Testing of Aging Aircraft Wiring." *IEEE Transactions on Electromagnetic Compatibility* 45 (2): 306–15. https://doi.org/10.1109/TEMC.2003.811305.

Gazdzinski, R.F., W.M. Denny, G.J. Toman, and R.T. Butwin. 1996. *Aging Managment Guideline for Commercial Nuclear Power Plants - Electrical Cable and Terminations*. Sandia National Labs SAND96-0344. Albuquerque, NM. https://www.nrc.gov/docs/ML0311/ML031140264.pdf.

Glass, S. W., A. M. Jones, L. S. Fifield, and T. S. Hartman. 2017. "Frequency Domain Reflectometry NDE for Aging Cables in Nuclear Power Plants." In *AIP Conference Proceedings* 1806, 080015. https://doi.org/10.1063/1.4974640.

Glass, S.W., Leonard S. Fifield, D. Gerges, T. Jonathan, A.M. Jones, and T.S. Hartman. 2015. *State of the Art Assessment of NDE Techniques for Aging Cable Management in Nuclear Power Plants*. Pacific Northwest National Laboratory PNNL-24649. Richland, WA. https://doi.org/10.2172/1242348.

Glass, S.W., A.E. Holmes, Leonard S. Fifield, and K.K. Anderson. 2020. *Assessment of EPRI's Tan Delta Approach to Manage Cables in Submerged Environments: Statistical Review of EPRI Data*. Pacific Northwest National Laboratory PNNL-28542-1. Richland, WA. https://doi.org/10.2172/1713064.

Glass, S.W., A.M. Jones, Leonard S. Fifield, and T.S. Hartman. 2016. *Bulk and Distributed Electrical Cable Non-Destructive Examination Methods for Nuclear Power Plant Cable Aging Management Programs*. Pacific Northwest National Laboratory PNNL-25634. Richland, WA. https://doi.org/10.2172/1328060

Glass, S.W., A.M. Jones, Leonard S. Fifield, T.S. Hartman, and Nicola Bowler. 2017. *Physics-Based Modeling of Cable Insulation Conditions for Frequency Domain Reflectometry (FDR)*. Pacific Northwest National Laboratory PNNL-26493. Richland, WA. http://www.pnnl.gov/main/publications/external/technical_reports/PNNL-26493.pdf

Glass, S.W., Mychal P. Spencer, M. Prowant, A. Sriraman, J. Son, and Leonard S. Fifield. 2023. "The ARENA Test Bed - A Versatile Resource for I&C Development and Validation." In *13th Nuclear Plant Instrumentation, Control & Human-Machine Interface Technologies*. Knoxville, TN, USA.

Glass, S.W., Mychal P. Spencer, A. Sriraman, Leonard S. Fifield, and M. Prowant. 2021. *Nondestructive Evaluation (NDE) of Cable Moisture Exposure Using Frequency Domain Reflectometry (FDR).* Pacific Northwest National Laboratory PNNL-31934. Richland, WA. https://doi.org/10.2172/1820614

Glass, S.W., A. Sriraman, M. Prowant, Mychal P. Spencer, Leonard S. Fifield, and S. Kingston. 2022. *Nondestructive Evaluation (NDE) of Cable Anomalies Using Frequency Domain Reflectometry (FDR) and Spread Spectrum Time Domain Reflectometry (SSTDR)*. Pacific Northwest National Laboratory PNNL-33334.

Glossary, Gartner. 2023. “Digital Twin Definition.” 2023. https://www.gartner.com/en/information-technology/glossary/digital-twin.

Imperatore, M. V., L. S. Fifield, D. Fabiani, and N. Bowler. 2017. “Dielectric Spectroscopy on Thermally Aged, Intact, Poly-Vinyl Chloride/Ethylene Propylene Rubber (PVC/EPR) Multipolar Cables.” In *2017 IEEE Conference on Electrical Insulation and Dielectric Phenomenon (CEIDP)*, 173–76. IEEE. https://doi.org/10.1109/CEIDP.2017.8257522.

IAEA. 2012. *Assessing and Managing Cable Ageing in Nuclear Power Plants.* International Atomic Energy Agency Nuclear Energy Series No. NP-T-3.6. Vienna, Austria. https://www-pub.iaea.org/MTCD/Publications/PDF/Pub1554_web.pdf

Joskow, P. L. 2006. *The Future of Nuclear Power in the United States: Economic and Regulatory Challenges.* Massechusetts Institute of Technology MIT-CEEPR 06-019WP. Cambridge, MA https://ceepr.mit.edu/wp-content/uploads/2023/02/2006-019.pdf

Kakimoto, A., E. Akihiro, H. Kaoru, and S. Nonaka. 1987. “Precise Measurement of Dielectric Properties at Frequencies from 1 KHz to 100 MHz.” *Review of Scientific Instruments* 58 (2): 269–75. https://doi.org/10.1063/1.1139320.

Pan, C., A. P. S. Gaur, M. Lynn, M. P. Olson, G. Ouyang, and J. Cui. 2022. “Enhanced Electrical Conductivity in Graphene–Copper Multilayer Composite.” *AIP Advances* 12 (1): 015310. https://doi.org/10.1063/5.0073879.

Spencer, M. P., A. Sriraman, M. Prowant, S.W. Glass, and L. S. Fifield. 2023. “Effect of Measurement Temperature on Electrical Cable Frequency Domain Reflectometry Response.” *Conference on Electrical Insulation and Dielectric Phenomena (CEIDP)*. IEEE

Sriraman, A., N. Bowler, S.W. Glass, and L. S. Fifield. 2018. “Dielectric and Mechanical Behavior of Thermally Aged EPR/CPE Cable Materials.” In *2018 IEEE Conference on Electrical Insulation and Dielectric Phenomena (CEIDP)*, 598–601. IEEE. https://doi.org/10.1109/CEIDP.2018.8544855.

Subudhi, M. 1996. *Literature Review of Environmental Qualification of Safety-Related Electric Cables*. Brookhaven National Laboratory NUREG/CR-6384 Vol.1 Part 2. Upton, NY. https://www.nrc.gov/docs/ML0316/ML031600732.pdf

Wikipedia. 2023. “Digital Twin.” 2023. https://en.wikipedia.org/wiki/Digital_twin.